Identification and characterization of microRNAs in oilseed rape (*Brassica napus*) responsive to infection with the pathogenic fungus *Verticillium longisporum* using *Brassica* AA (*Brassica rapa*) and CC (*Brassica oleracea*) as reference genomes

Dan Shen[1], Ina Suhrkamp[1], Yu Wang[2], Shenyi Liu[3], Jan Menkhaus[1], Joseph-Alexander Verreet[1], Longjiang Fan[2] and Daguang Cai[1]

[1]Department of Molecular Phytopathology and Biotechnology, Institute of Phytopathology, Christian Albrechts University of Kiel, Hermann Rodewald Str. 9, D-24118 Kiel, Germany; [2]Department of Agronomy, James D. Watson Institute of Genome Sciences & Institute of Bioinformatics, Zhejiang University, Hangzhou 310058, China; [3]Oil Crops Research Institute, Chinese Academy of Agricultural Sciences, Wuhan 430062, China

Authors for correspondence:
Daguang Cai
Tel: +49 431 8803215
Email: dcai@phytomed.uni-kiel.de

Longjiang Fan
Tel: +86-571-88982730
Email: fanlj@zju.edu.cn

Received: *22 May 2014*
Accepted: *5 June 2014*

New Phytologist (2014)
doi: 10.1111/nph.12934

Key words: *Brassica napus*, miR168-AGO1, microRNAs, plant–fungus interaction, *Verticillium longisporum*.

Summary

- *Verticillium longisporum*, a soil-borne pathogenic fungus, causes vascular disease in oilseed rape (*Brassica napus*). We proposed that plant microRNAs (miRNAs) are involved in the plant–*V. longisporum* interaction.
- To identify oilseed rape miRNAs, we deep-sequenced two small RNA libraries made from *V. longisporum* infected/noninfected roots and employed *Brassica rapa* and *Brassica oleracea* genomes as references for miRNA prediction and characterization.
- We identified 893 *B. napus* miRNAs representing 360 conserved and 533 novel miRNAs, and mapped 429 and 464 miRNAs to the AA and CC genomes, respectively. Microsynteny analysis with the conserved miRNAs and their flanking protein coding sequences revealed 137 AA–CC genome syntenic miRNA pairs and 61 AA and 42 CC genome-unique miRNAs. Sixty-two miRNAs were responsive to the *V. longisporum* infection. We present data for specific interactions and simultaneously reciprocal changes in the expression levels of the miRNAs and their targets in the infected roots. We demonstrate that miRNAs are involved in the plant–fungus interaction and that miRNA168-Argonaute 1 (AGO1) expression modulation might act as a key regulatory module in a compatible plant–*V. longisporum* interaction.
- Our results suggest that *V. longisporum* may have evolved a virulence mechanism by interference with plant miRNAs to reprogram plant gene expression and achieve infection.

Introduction

Verticillium longisporum, a soil-borne pathogenic fungus, causes vascular disease in oilseed rape (*Brassica napus*) (Zeise & von Tiedemann, 2002). Fungal hyphae enter the host through the roots without developing specific infection structures, and grow intra- and intercellularly through the root cortex toward the central cylinder. The fungus spreads systemically in the plant either by hyphal growth or through the conidia transported from infected roots to shoots with the transpiration stream. Fungal colonization of xylem vessels drastically affects the xylem function, resulting in the obstruction of the transpiration stream, and restricts water and nutrient transportation (Eynck *et al.*, 2007; Floerl *et al.*, 2008). Typical symptoms include stunted growth, leaf chlorosis and enhanced plant senescence in the foliage as well as reduced leaf area and early flowering. Symptoms in winter oilseed rape plants occur late in the growing season, after flowering and during ripening (Eynck *et al.*, 2009). *Verticillium longisporum* resistance is not currently present in the *B. napus* gene pool. Molecular understanding of the plant–*V. longisporum* interaction will be helpful for the development of control strategies against *V. longisporum*.

The plant–*V. longisporum* interaction represents a unique system for studying plant–fungus interactions, and has been intensively investigated with *Arabidopsis thaliana* (Floerl *et al.*, 2010, 2012). Genetic studies identified the *Verticillium dahliae*-tolerance 1 (*VET1*) locus conferring development-dependent tolerance (Veronese *et al.*, 2003). Root transcriptome analysis revealed that the plant–*V. longisporum* interaction involves a rapid reprogramming of plant gene expression (Iven *et al.*, 2012). The plant hormone ethylene (ET) appears to be important for *V. longisporum* colonization in plants, as the *etr1-1* receptor mutant shows reduced *V. longisporum*-induced symptoms (Veronese *et al.*, 2003; Johansson *et al.*, 2006). Ralhan *et al.* (2012)

demonstrated that the fungus requires a functional jasmonic acid-independent CORONATINE INSENSITIVE1 (COI1) receptor in roots to elicit disease symptoms in *A. thaliana* shoots. Plant-derived signals stimulate the expression of functional catalase peroxidase in *V. longisporum*, which is required for the late phase of disease (Singh *et al.*, 2012).

Small RNA (sRNA) directed RNA-induced silencing complex (RISC) activities regulate many biological pathways in plants (Palatnik *et al.*, 2003; Laufs *et al.*, 2004; Lauter *et al.*, 2005; Ruiz-Ferrer & Voinnet, 2009). There are two potential mechanisms of sRNA–mediated gene regulation: RNA endonucleolytic cleavage at the center of sRNA–target hybrids and translation repression (Bartel, 2004; Jones-Rhoades *et al.*, 2006; Iwakawa & Tomari, 2013), which is also termed post-transcriptional gene silencing (PTGS). As a major class of sRNAs, microRNAs (miRNAs) are generated from intronic or intergenic regions by RNA polymerase II, processed into pre-miRNAs by the Dicer-like 1 (DCL1)/HYPONASTIC LEAVES1 (HYL1)/SERRATE (SE) protein and then diced as an miRNA–miRNA* duplex. One selected strand of the duplex is incorporated in the Argonaute (AGO) protein, a catalytic component of RISC, to execute their function in regulating gene expression (Vazquez *et al.*, 2010; Naqvi *et al.*, 2012).

There is increasing evidence that the modulation of miRNA levels plays an important role in reprogramming plant responses to various stresses, including nutrient deficiency, drought, cold, salinity, and mechanical stress (Jones-Rhoades & Bartel, 2004; Aung *et al.*, 2006; Bari *et al.*, 2006; Sunkar *et al.*, 2006), and in plant–pathogen interactions. MiR393 was induced by a bacterial Pathogen-associated molecular pattern (PAMP) (flg22) and targeted the genes encoding the auxin receptors transport inhibitor response 1 (*TIR1*), auxin signaling F-box protein 2 (*AFB2*) and *AFB3*, negatively regulating auxin signaling (Navarro *et al.*, 2006). MiR156 and miR164 were induced by viral infection in *Arabidopsis thaliana* and tobacco (*Nicotiana tabacum*) (Kasschau *et al.*, 2003). Bra-miR158 and bra-miR1885 from *Brassica rapa* (Bra) were highly specific to Turnip mosaic virus (TuMV) infection and targeted a Toll/interleukin receptor domain-containing (TIR)–Nucleotide-binding site (NBS)–Leucine-rich repeat (LRR)–disease resistance (R) protein (He *et al.*, 2008). MiR6019 and miR6020 from tobacco were demonstrated to guide cleavage of transcripts of the *N* gene that confers resistance to Tobacco mosaic virus (TMV) (Li *et al.*, 2012). In *A. thaliana*, miR396 acted as a key regulator for reprogramming of root cells during cyst nematode infection (Hewezi *et al.*, 2012).

Also, the effect of PTGS on the plant–*Verticillium* interaction has been demonstrated by analysis of the *A. thaliana* gene silencing mutants *suppressor of gene silencing 2* (*sgs2*), *sgs3*, *AGO1, ARGONAUTE 7* (*ago7*) and *DICER-LIKE 4* (*dcl4*), which are all involved in sRNA synthesis and exhibit enhanced susceptibility, with the exception of *ago1* mutants, which develop fewer symptoms (Ellendorff *et al.*, 2009). *AGO1* encodes the RNA slicer enzyme of the miRNA pathway which is targeted by miR168. Several studies have shown the involvement of AGO1 in plant antiviral defense (Morel *et al.*, 2002; Qu *et al.*, 2008; Várallyay *et al.*, 2010) and PAMP/pattern-triggered immunity (PTI) responses (Li *et al.*, 2010). Weiberg *et al.* (2013) demonstrated that the *Botrytis cinerea* sRNA effector hijacks AGO1 to achieve infection. Also, the vascular-related NAC (NAM, ATAF1,2 and CUC2) domain transcription factors VASCULAR-RELATED NAC-DOMAIN 6 (VND6) and VND7 were identified in *V. longisporum*-induced transdifferentiation of *de novo* xylem formation (Reusche *et al.*, 2012). NAC transcription factors are known targets of miR164 (Rhoades *et al.*, 2002). The role of miRNAs in the plant–*V. longisporum* interaction is, however, poorly understood.

Although massive parallel deep-sequencing technology has greatly accelerated the identification of sRNAs, lacking in genome sequence information strongly limits research on miRNAs in many crop plants. *Brassica napus* is one of the most economically important crops world-wide, but its whole genome has not yet been sequenced. Genome-wide identification and characterization of miRNAs in *B. napus* remain a great challenge. Currently, miRBase (release 20; http://www.mirbase.org/) lists only 92 mature miRNAs in *B. napus*, seven miRNAs in *Brassica oleracea* and 43 miRNAs in *Brassica rapa*. Most of these were identified on the basis of expressed sequence tag (EST) and tentative consensus (TC) sequences (Yu *et al.*, 2012; Zhao *et al.*, 2012) and data on their genome localization and organization are completely lacking. Thus, the draft genome sequences of *B. rapa* accession Chifu-401-42 (Wang *et al.*, 2011) and *B. oleracea* (Liu *et al.*, http://www.oilcrops.cn/contact.aspx?code=00200007&id= 809) offer the possibility of genome-wide identification and characterization of oilseed rape miRNAs as well as exploration of their evolution.

To explore the role of miRNAs in the oilseed rape–*V. longisporum* interaction, we analyzed two sRNA libraries from mock-infected and *V. longisporum*-infected oilseed rape roots by deep sequencing. Using *Brassica* AA (*B. rapa*) and CC (*B. oleracea*) as references for the corresponding subgenomes of *B. napus*, we identified 893 *B. napus* miRNAs, which represent 360 conserved and 533 novel miRNAs, with a high confidence. In addition, a microsynteny analysis performed on the miRNAs and their flanking protein coding sequences provides new insights into the possible origin and evolution of oilseed rape miRNAs. By comparison of miRNAseq data between two libraries and by systemic expression profiling analysis, we identified a set of miRNAs highly responsive to *V. longisporum* infection. We present data supporting the idea that plant miRNAs are involved in the plant–fungus interaction and that miRNA168-AGO1 expression modulation may act as a key regulatory module in the plant–*Verticillium* interaction.

Materials and Methods

Plant material, pathogenic infection and small RNA sequencing

Seeds of oilseed rape (Express 617; *Brassica napus* L.) were surface-sterilized and plated on B5 medium for germination. A conidia suspension of *Verticillium longisporum* (VL43) was harvested from potato dextrose broth (PDB) by filtering through sterilized gauze. Ten-day-old plants were extracted from B5 medium and the root parts were placed in the

conidia suspension (1×10^7 conidia ml^{-1}) and water as mock inoculation for 30 min. Inoculated plants were replanted into 2×2 cm plastic tubes containing sterilized soil and sand. All plants were placed in a climatic cabinet with a 16-h photoperiod. At 6 and 12 d post-infection (dpi), plant roots were collected for RNA extraction.

Total RNA was isolated using Trizol reagent (Invitrogen, Darmstadt, Germany) according to the manufacturer's instructions. The quality of RNA was controlled using the Agilent 2100 Bioanalyzer (Agilent, Böblinge, Germany). Total RNA from 6-dpi roots was mixed for sequencing. In total, two samples, untreated roots (UR) and *V. longisporum*-infected roots (IR), were used to construct sRNA libraries. Small RNA sequences were generated using Illumina's Solexa sequencing technology (BGI, Beijing, China).

Data analysis

Identification of candidate miRNAs All sRNA reads, referred to as raw reads, were processed to remove adaptors, low-quality tags and contaminants. Clean reads were then mapped to the *Brassica rapa* (AA genome) (Wang *et al.*, 2011; http://www.brassicadb.org) and *Brassica oleracea* (CC genome) (Liu *et al.*: http://www.oilcrops.cn/contact.aspx?code=00200007&id= 809) genomes, respectively. Only reads with perfect genomic matches were processed for further miRNA and small interfering RNA (siRNA) annotation. After removing unexpected sRNA, such as ribosomal RNA (rRNA), transfer RNA (tRNA), small nuclear RNA (snRNA), small nucleolar RNA (snoRNA) and degraded mRNA by aligning clean reads to GenBank, Rfam (10.1), *B. rapa* and *B. oleracea* mRNA databases, the sRNA sequences were subject to secondary hairpin structure prediction using Mireap (http://sourceforge.net/projects/mireap/). The resulting structures with < -18 kcalmol^{-1} free energy, < 300 nt spaces between miRNA and its complementary sequence miRNA*, and > 16 nt matched nucleotides but < 4 nt bulge of miRNA and miRNA* were retained as miRNA candidates. The conservation status of the candidates was analyzed by comparison with all plant miRNAs recorded in miRBase (release 20). All miRNA sequence data obtained are available from Gene Expression Omnibus (http://www.ncbi.nlm.nih.gov/geo/; accession number GSE58322).

Identification and enrichment analysis of miRNA target genes Targets of each candidate miRNA were predicted using web server psRNATarget (http://plantgrn.noble.org/psRNATarget/, Dai & Zhao, 2011). *Brassica rapa* and *B. oleracea* transcripts were included in the prediction. The predicted targets with default parameters were processed in Gene Ontology (GO) enrichment analysis and Kyoto Encyclopedia of Genes and Genomes (KEGG) pathway analysis (http://www.genome.jp/kegg/) which were performed using Blast2GO (http://www.blast2go.com/b2ghome; Conesa & Götz, 2008).

Genomic synteny of miRNAs between *B. rapa* and *B. oleracea* genomes miRNA orthologs between *B. rapa* and *B. oleracea* were analyzed using a microsynteny-based method (Ma *et al.*, 2010). For each miRNA, its 10 flanking protein-coding loci were retrieved from the *B. rapa* and *B. oleracea* genomes, respectively. Homology tests of *MIRNA* and flanking genes between the *B. rapa* and *B. oleracea* genomes were performed using BLASTn and the top five hits for each *MIRNA* were chosen for flanking locus tests. A syntenic miRNA pair between *B. rapa* and *B. oleracea* was defined with at least one identical upstream or downstream flanking protein-coding gene. Syntenic miRNAs were divided into four sets: (1) miRNAs for which the MIRNA hit had maximally preserved synteny in both upstream and downstream genes; (2) miRNAs for which the MIRNA hit maintained the synteny with only upstream or downstream genes; (3) miRNAs for which none of the top five hits of MIRNA showed synteny with the 10 flanking genes, and (4) miRNAs that were uniquely identified in the *B. rapa* genome or *B. oleracea* genome. The first three sets were taken to be syntenic miRNAs for construction of the circos map (Krzywinski *et al.*, 2009).

Transcript analysis of miRNAs and target genes

Low-molecular-weight (LMW) RNA was enriched by 50% PEG (MW = 8000) and 5 M NaCl precipitation as described previously (Lu *et al.*, 2007). Mature miRNA expression analysis was performed by stem-loop RT-PCR, as described by Chen *et al.* (2005). For cDNA synthesis, 200 ng of LMW RNA from each sample was reverse-transcribed using the SuperScript™ First-Strand Synthesis System III (Invitrogen) with U6 snRNA as the internal control. The PCR consisted of an initial 3-min denaturation step at 94°C followed by 40 cycles of 30 s at 94°C, 30 s at 60°C and 30 s at 72°C. The amplifications use the corresponding miRNA sequence as the sense primer and the stem-loop universal primer as the antisense primer. The PCR product was checked on 12% polyacrylamide/urea gel and defined using a 10-bp DNA ladder (O'Range Ruler; Thermo Scientific, Schwerte, Germany). For cDNA synthesis of predicted targets, 2 μg of total RNA of each sample was used. Quantitative PCR (qPCR) reactions were performed in a 7300 Real Time PCR System (Applied Biosystems) with MAXIMA® SYBR Green Master Mix (Fermentas, Schwerte, Germany) and β-tubulin as the reference gene. Invariant expression of the β-tubulin gene in response to *V. longisporum* infection was confirmed beforehand. The mRNA levels for each cDNA probe were normalized with respect to the β-tubulin message (Rietz *et al.*, 2012). The relative fold changes in expression of miRNAs and related genes were calculated using the comparative threshold cycle (Ct) method (Livak & Schmittgen, 2001). All the reactions were performed in triplicate with three independent experiments. The primer pairs are listed in Supporting Information Tables S1 and S2.

RNA ligase-mediated 5′ rapid amplification of cDNA ends (RLM-5′ RACE) analysis

5′ rapid amplification of cDNA ends (RACE) was carried out for validation of predicted targets of miRNAs using the GeneRacer TM Kit (Invitrogen) with 2 μg of total RNA. The first two steps of dephosphorylation of RNA and removal of the mRNA

cap structure were not carried out; the procedure started with ligation of the RNA oligo to the mRNA followed by reverse transcription of mRNA using the random primers. For amplifying cDNA ends, a gene-specific primer was designed (Table S3). Temperature cycling conditions for touchdown PCR were as follows: 2 min at 94°C, followed by five cycles of 30 s at 94°C and 90 s at 72°C, five cycles of 30 s at 94°C and 120 s at 70°C, and 25 cycles of 30 s at 94°C, 30 s at 65°C and 90 s at 72°C and finally 10 min at 72°C. One microliter of this initial touchdown PCR was the template for the following nested PCR: 2 min at 94°C, followed by 25 cycles of 30 s at 94°C, 30 s at 65°C and 2 min at 72°C and finally 10 min at 72°C. The reaction products were separated on a 1.2% agarose gel, purified and cloned into the pGEM-T vector (Promega, Mannheim, Germany) for sequencing. Sequencing results were aligned using CLUSTALW (Thompson *et al.*, 1994).

Inoculation of *A. thaliana* plants

Seeds of the *A. thaliana miR168b* mutant (SALK_094145; http://signal.salk.edu/) and the AGO1 mutants *ago1-t* (SALK_021251), *ago1-25* and *ago1-27* (kindly provided by Prof. Hervé Vaucheret, Laboratoire de Biologie Cellulaire, INRA, Versailles Cedex, France) were surface-sterilized and sown in a 1 : 1 sand : soil mixture under a photoperiod with 8 h light : 16 h dark. Three-week-old plants were up-rooted and incubated by dipping for 15 min in a conidial suspension of VL43 (10^6 spores ml^{-1}) or in water for the mock inoculation. Subsequently, plants were replanted in single pots containing sterilized soil, and 1 ml of conidial suspension or water was added to each pot; plants were then kept under a transparent cover for 4 d to maintain humidity. The homozygosity of *A. thaliana* mutants was confirmed beforehand (by the Salk Institute Genomic Analysis Laboratory, http://signal.salk.edu).

Quantification of *V. longisporum* DNA

For *V. longisporum* biomass quantification in *A. thaliana* plants, whole rosettes of plants were used. Total DNA was extracted using Nucleospin Plant II (Macherey-Nagel, Düren, Germany). Amplification and quantification of *V. longisporum* and *A. thaliana* DNA were performed with primers OLG70 (CAGCGAAACGCGATATGTAG) and OLG71 (GGCTTGT AGGGGGTTTAGA), and ACT1 (ACCTTGCT GGACGTGA CCTTACTGAT) and ACT2 (GTTGTCTCGT GGATTCCA GCAGCTT), respectively (Reusche *et al.*, 2012). Standard curves for the relationship between the amount of DNA and the Ct value of the two primers were determined with pure *V. longisporum* and *A. thaliana* DNA. The qPCR program consisted of a 95°C denaturation step for 5 min, followed by 35 cycles of 15 s at 95°C, 35 s at 56°C and 35 s at 72°C and finally 10 min at 72°C. The amount of *V. longisporum* DNA was normalized by *A. thaliana* DNA. Pools of three plants were analyzed per time-point, with three repetitions. Statistical analyses were performed using ANOVAs.

Results

Identification of small RNAs by deep sequencing

To identify sRNAs produced in response to *V. longisporum* infection, two sRNA libraries were constructed from the *B. napus* roots treated with *V. longisporum* infection (IR) and with mock infection (UR), respectively, and sequenced by deep sequencing. In total, 16 926 646 (5085 622 unique) and 17 157 110 (4223 911 unique) reads 18–44 nt in size were obtained from the mock-infected and *V. longisporum*-infected roots, respectively (Table 1). In both the UR and IR libraries, a major proportion of the sRNAs were of size 21–24 nt, most of which were 24-nt sRNAs (Fig. S1). From the reads, 45.9% and 43.8% of unique reads could be mapped to the *Brassica* AA and CC genomes, respectively. After removing tRNAs, rRNAs, snRNAs, snoRNAs, repeat-associated small interfering RNAs (rasiRNAs) and degraded mRNAs, other reads were referred to as endogenous sRNAs for further analysis. In agreement with previous reports, a dominant nucleotide preference for adenosine (A) at the 5′ first position of 24-nt sRNAs (57%) and at the end position of 23-nt sRNAs (53%) was observed in our sRNA populations (Fig. S2). A significant nucleotide preference for thymine (T) at the 3′ second position of 23-nt sRNAs was observed, which was found in 49% of 23-nt mapped sRNAs in this study (Fig. S2).

Identification of *B. napus* miRNAs

To identify miRNAs in *B. napus*, we applied the strategy of employing the whole genomes of two *B. napus* progenitors,

Table 1 Small RNAs from *Brassica napus* roots

	UR		IR	
	Unique	Abundant	Unique	Abundant
Total number of reads	5085 622	16 926 646	4223 911	17 157 110
Mapped to *B. rapa or B. oleracea* genome	2335 615 (45.9%)	9899 731 (58.5%)	1851 246 (43.8%)	8354 172 (48.7%)
B. rapa	1192 848 (23.5%)	7107 303 (42.0%)	955 669 (22.6%)	6109 185 (35.6%)
B. oleracea	1820 776 (35.8%)	8797 610 (52.0%)	1443 201 (34.2%)	7369 932 (43.0%)
Mapped to *B. rapa* or *B. oleracea* transcripts	474 831 (9.3%)	1510 735 (8.9%)	379 536 (9.0%)	1125 027 (6.6%)
B. rapa	267 038 (5.3%)	855 763 (5.1%)	214 143 (5.1%)	633 906 (3.7%)
B. oleracea	301 118 (5.2%)	1021 962 (6.0%)	242 075 (5.7%)	760 040 (4.4%)

UR, untreated roots (mock-infected); IR, *Verticillium longisporum*-infected roots.

Table 2 Conserved and novel microRNAs (miRNAs) newly identified in *Brassica napus*

miRNA family	miRNA	Mature sequence	Read number	
			UR	IR
miR156	bna-miR156h-ad	TGACAGAAGAGAGTGAGCAC	453 894	504 555
	bna-miR156ae	CGACAGAAGAGAGTGAGCAC	1123	979
	bna-miR156af-ai	TTGACAGAAGAAAGAGAGCAC	3978	5195
	bna-miR156aj	TGACAGAAGAGAGAGAGCAC	628	758
	bna-miR156ak	TGACAGAAGAGAGGGAGCAC	2238	2523
	bna-miR156al	TTGACAGAAGAGAGCGAGCAC	3873	2698
	bna-miR157a-e	TTGACAGAAGATAGAGAGCAC	859 570	726 476
miR158	bna-miR158a,b,d	TCCCAAATGTAGACAAAGCA	11 991	11 279
	bna-miR158c.1	TTTCCAAATGTAGACAAAGCA	29 276	23 055
	bna-miR158c.2	CTTTGTCTATCGTTTGGAAAAG	49 625	74 886
miR159	bna-miR159a,b.1,c,d.1,e	TTTGGATTGAAGGGAGCTCTA	1019	634
	bna-miR159b.2,d.2	CTTGCATATCTTAGGAGCTTT	144	169
	bna-miR319a-e	TTGGACTGAAGGGAGCTCCCT	111	45
miR160	bna-miR160e-n	TGCCTGGCTCCCTGTATGCCA	2399	732
miR161	bna-miR161a	TCAATGCACTGAAAGTGACTA	186	160
miR162	bna-miR162b-f	TCGATAAACCTCTGCATCCAG	954	537
miR164	bna-miR164g-i	TGGAGAAGCAGGGCACGTGCA	10 479	4005
	bna-miR164e-f	TGGAGAAGCAGGGCACGTGCG	2199	732
miR166	bna-miR165a-f	TCGGACCAGGCTTCATCCCCC	28 731	19 391
	bna-miR166g-n	TCGGACCAGGCTTCATTCCCC	54 782	38 322
miR167	bna-miR167e-h	TGAAGCTGCCAGCATGATCTA	50 430	34 187
	bna-miR167i	TGAAGCTGCCAGCATGATCT	405	138
	bna-miR167j	TAAGCTGCCAGCATGATCTTG	610	344
	bna-miR167k	TGAAGCTGCCAGCATGATCTT	14 021	10 511
miR168	bna-miR168c-f	TCGCTTGGTGCAGGTCGGGAA	64 053	39 103
	bna-miR168g-i	TCGCTTGGTGCAGGTCGGGAC	104 182	18 466
miR169	bna-miR169ab.1,ac-af	CAGCCAAGGATGACTTGCCGG	1354	444
	bna-miR169ab.2	TGAAGTGGAGTAGAGTATAATG	450	562
	bna-miR169ag-ap	TGAGCCAAAGATGACTTGCCG	11769	8655
	bna-miR169aq,ar	TGAGCCAAAGATGACTTGTCG	166	60
	bna-miR169as	TGAGCCAAGGATGACTTGCCG	120	175
	bna-miR169ba.1	AGCCAAGGATGACTTGCCGG	214	175
	bna-miR169ba.2	TGAAGGAATAGAGAGTGGAAT	2590	1810
miR172	bna-miR172e-j	AGAATCTTGATGATGCTGCAT	1123	1972
	bna-miR172k-q	GGAATCTTGATGATGCTGCAT	154	160
miR390	bna-miR390d-k	AAGCTCAGGAGGGATAGCGCC	6239	2863
miR391	bna-miR391a-c	TTCGCAGGAGAGATAGCGCCA	255	238
miR396	bna-miR396d,e	TTCCACAGCTTTCTTGAACTG	674	423
miR397	bna-miR397c	TCATTGAGTGCAGCGTTGATGT	1265	1062
miR400	bna-miR400b-e	TATGAGAGTATTATAAGTCAC	200	157
miR408	bna-miR408	ATGCACTGCCTCTTCCCTGGC	167	97
miR827	bna-miR827a-c	TTAGATGACCATCAACAAATA	1531	1428
miR1885	bna-miR1885a-c	CATCAATGAAAGGTATGATTCC	184	406
miR5654	bna-miR5654a-c	ATAAATCCCAAGCATCATCCA	4878	2401
miR5716	bna-miR5716a	TTGGATAAGTGAAGATATAAA	278	243
miR6029	bna-miR6029a	TGGGGTTGTGATTTCAGGCTT	848	848
miR6030	bna-miR6030a,b	TCCACCCATACCATACAGACCC	357	326
novel_miRX1	novel_miRX1.1,2	GTCTGGGTGGTGTAGTCGGTT	446	97
novel_miRX19	novel_miRX19.1	TTGCTATAGATGGTTTCTGCT	428	424
novel_miRX48	novel_miRX48.1	GGATGGTCACCAGTCGGACCCTA	261	189
novel_miRX65	novel_miRX65.1	TGGGATAGCAGGACACTCATA	179	70
novel_miRX78	novel_miRX78.1	CTGTAAGTAGAAGTATATGGATA	211	169
novel_miRX79	novel_miRX79.1	AGGGAACAGAGCAAGCGGGTT	156	122
novel_miRX103	novel_miRX103.1	TGGACGACTTAGTAGATGACTT	142	151
novel_miRX136	novel_miRX136.1-3	TTTCGGCTAAGAGACGGTTCTTA	229	145
novel_miRX168	novel_miRX168.1	GTCGGTATGTCGTCGGAATAACA	200	205
novel_miRX199	novel_miRX199.1-6	ATATGTAGAGATTTTTGTTACTA	171	127
novel_miRX227	novel_miRX227.1	TGACCGAGTAGACCGATAGTC	1530	2301
novel_miRX230	novel_miRX230.1	TAAAAGCTAAGAGACTGTATC	178	223
novel_miRX249	novel_miRX249.1,2	TCTTGACGACGGTGCTTTTGA	1005	507

Table 2 (Continued)

miRNA family	miRNA	Mature sequence	Read number	
			UR	IR
novel_miRX259	novel_miRX259.1,2	TCAAACTTGAGGTGGTCTGGATA	193	129
novel_miRX270	novel_miRX270.1,2	ACTTATAATTAAGTCGTCTGG	168	91
novel_miRX280	novel_miRX280.1,2	AAGACTGTAAAATCTAATTGGTT	117	149
novel_miRX300	novel_miRX300.1-3	ATTGGTTGAATTGTAGTTAGGTA	155	133
novel_miRX317	novel_miRX317.1,2	TTGAAGCGATTTGTAGCGGTTTA	1171	1131
novel_miRX332	novel_miRX332.1,2	GTGGACGTGCCGGAGTGGTTA	405	202
novel_miRX345	novel_miRX345.1,2	TTGTGCACATGTGGATAGGCTTA	1115	923
novel_miRX355	novel_miRX355.1,2	TTGTAGAATTTTGGGAAGGGC	769	879

UR, untreated roots (mock-infected); IR, *Verticillium longisporum*-infected roots.
Only highly expressed miRNAs (> 100 reads in one sample) are shown.

B. rapa (AA) and *B. oleracea* (CC), as references for miRNA prediction. We identified 893 nonredundant miRNA precursors (GSE58322) from the two species, which are able to form a perfect hairpin structure as expected by miRNA or miRNA*. Of these, 429 were from the AA genome and 464 from the CC genome (Tables S4, S5). By comparison with known plant miRNAs in the miRBase (release 20), 360 conserved (Table S4) and 533 novel miRNAs (named Bna-novel_miRXx.x in this study) (Table S5) were identified (highly expressed conserved and novel miRNAs are listed in Table 2). In addition to 45 known *B. napus* miRNAs in the current miRBase (release 20), 315 conserved miRNAs were newly identified in this study.

The complementary miRNA* sequences were detected for 230 (63.9%) conserved and 38 (7.1%) novel miRNAs (Tables S4 and S5). About one-fourth of miRNA* sequences showed accumulation that was almost equal to or even higher than that of the corresponding miRNAs, including the families miR169, miR171, miR396, miR2111 and miR408. miR408* accumulation was 40 times that of miR408, and miR171a*–c*,j*l* showed higher accumulation than miR171a–c,j,l in both libraries (Fig. S3). A similar observation for miR408 and miR171a–c,j,l in *B. napus* was reported by Zhao *et al.* (2012).

To confirm the predicted miRNAs, 39 conserved and eight novel highly expressed miRNA sequences were selected for stem-loop reverse transcription PCR analysis. Results summarized in Fig. S4 demonstrate the expression of 37 conserved miRNA sequences in both infected and control roots, except for bna-miR319a–e and bna-miR391a–c, which did not show RT-PCR products. All eight of the novel miRNAs were detectable in both samples (Fig. S4).

Synteny of miRNAs between AA and CC subgenomes

The availability of *B. rapa* (AA) and *B. oleracea* (CC) genomes allows investigation of the parental origin and evolution of *B. napus* miRNAs. We mapped 429 and 464 of the 893 predicted *B. napus* miRNAs to the AA and CC genomes, respectively, showing almost equal contributions of the two progenitors to the *B. napus* miRNAs (Table 3). To ascertain genomic synteny of the predicted miRNAs between the AA and CC subgenomes, a microsynteny analysis was performed with the miRNAs and their flanking protein-coding sequences (Tables 3, S6, S7). In total, 137 AA–CC syntenic conserved miRNA pairs were identified, which are scattered almost evenly throughout the chromosomes (Fig. 1, Table S6). The synteny was found in almost all conserved miRNA families, except for miR1511, miR1885, miR1863, miR4414, miR5067, miR862_2, miR5654, miR5721, miR6030 and miR6035, which are known as less conserved and less expressed miRNA families in plants. Consistent with this, the nonsynthetic miRNA families were found to have low to moderate abundance in both the IR and UR libraries, and their members to be present as single or low numbers of copies in the genomes (Table 2). Furthermore, 103 conserved miRNAs were AA/CC genome unique, including 61 for the AA genome and 42 for the CC genome. Several members of highly conserved miRNA families, for example, miR164a and miR164g, were unique to the AA genome but only miR160i was unique to the CC subgenome (Fig. 1). Only four syntenic miRNA pairs between the AA and CC subgenomes were found with novel miRNAs (Table S7).

Table 3 The origin of microRNAs (miRNAs) in the AA and CC genomes

Type		AA	CC
Conserved miRNA	Total	194	166
	Synteny miRNAs[a]	137	137
	Both loci	128	128
	Single loci	9	9
	Unique miRNAs	61	42
Novel miRNA	Total	235	298
	Synteny miRNAs[a]	4	4
	Both loci	4	4
	Single loci	0	0
	Unique miRNAs	216	282

aIncluding multi-syntenic miRNA pairs formed in the AA and CC subgenomes.

miRNA clusters were also identified in the *B. napus* genome. Almost identical precursors of miR169an and miR169ao were found to be clustered within a 22.6-kb genome region (Table S4, Fig. S5a). While miR156r, miR156s and miR156t are located in tandem within a 1-kb region of the AA genome, miR168j,

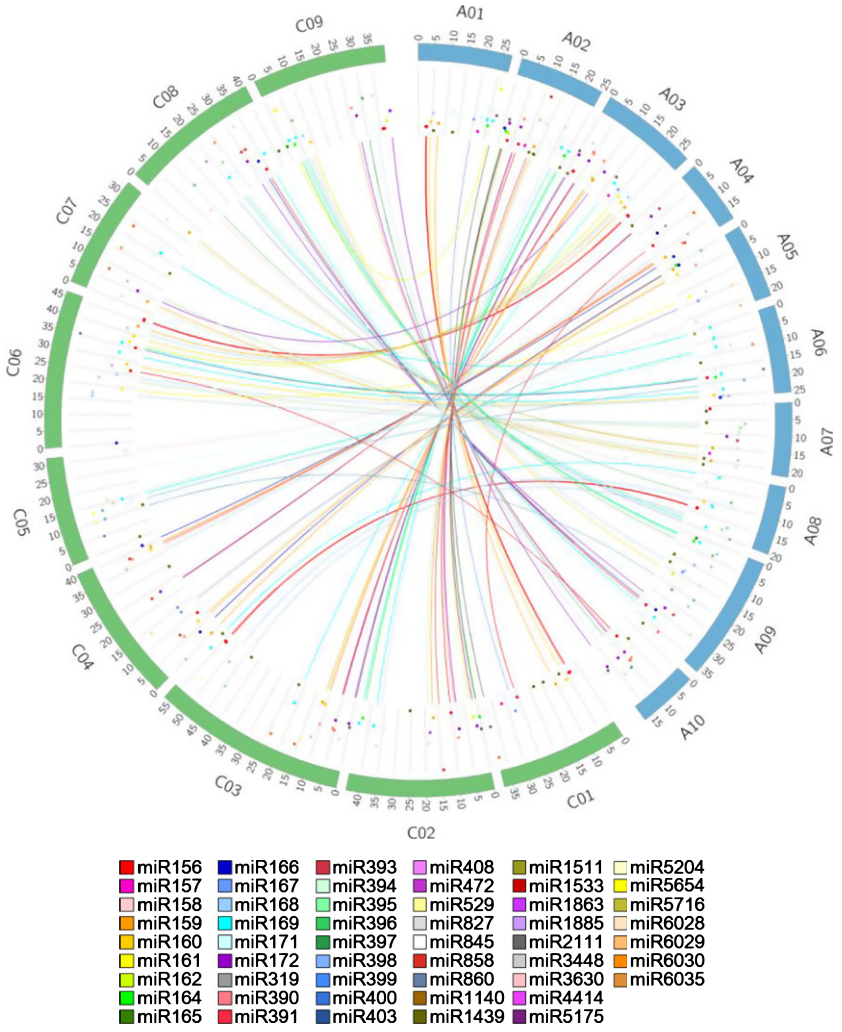

Fig. 1 Syntenic *MIRNA* loci of conserved microRNAs (miRNAs) between the *Brassica rapa* (AA) and *Brassica oleracea* (CC) genomes. Positions of annotated *MIRNA* loci are shown using dots that are color-coded according to the family. Links show synteny between *MIRNA* loci using the microsynteny-based method. A01–A10: chromosomes of *B. rapa*. C01-C09: chromosomes of *B. oleracea*.

miR168k, miR168l and miR168m reside in a 5-kb region of the CC genome. It is noteworthy that the clusters of miR156 and miR168 are not conserved between the AA and CC subgenomes (Table S4, Fig. S5b,c).

The whole-genome gene annotation revealed that most of the miRNAs (870) reside in intergenic regions and only 23 miRNAs reside in intragenic regions (Table 4). Strikingly, eight miRNAs are located within genes that are potential targets of the corresponding miRNAs. In agreement with the result reported by He *et al.* (2008) in *B. rapa*, we found that miR1885b resides within its target Bra027889, a TIR-NBS-LRR class resistance gene analog. Similar results were obtained for miR156aj, miR168a, miR393h, bna-novel-miRX9.2, bna-novel-miR71.1, bna-novel-miR265.1 and bna-novel-miR274.1 (Table 4).

Prediction and validation of miRNA targets

Because the target sites of plant miRNAs are predominantly located in the open reading frames (ORFs) of their targets (Rhoades *et al.*, 2002), we focused target prediction on coding sequences. For 360 conserved miRNAs, 475 and 452 targets were predicted for *B. rapa* and *B. oleracea*, respectively (Tables 5, S8–S11). No targets were predicted for miR1140a, miR169b, aw–az,ab.1,ac–af and miR4414b in *B. rapa* or for miR169d,f,aa, au,l,o–z, miR827a–c, miR6028a and miR4414b in *B. oleracea*. For 533 novel miRNAs, 1343 and 1271 targets were predicted, respectively, for *B. rapa* and *B. oleracea*, and 33 novel miRNAs did not have any targets in either species (Table S8–S11).

In agreement with the literature, the majority of potential targets for the conserved miRNAs are transcription factors and share high homology with *A. thaliana* orthologs (Table 5). For example, both miR160 and miR167, which target auxin response factor (ARF) transcription factors in *A. thaliana* (Mallory *et al.*, 2005; Wu *et al.*, 2006), as well as miR156/miR157 and miR162, which target squamosa promoter binding-like (SPL) protein and dicer-liker (DCL) protein in *A. thaliana*, are included in our prediction. Similar results were obtained for miRNA families miR159/miR319, miR164, miR165, miR168, miR171, miR172, miR393, miR394, miR395, miR397 and miR472. These data suggest that the miRNA–target interaction might be highly conserved between dicot and monocot plants In addition, we identified a subset of dicot-specific miRNA families, including miR158, miR400, miR472, miR858 and miR2111, which target pentatricopeptide repeat (PRR) protein,

Table 4 MicroRNAs (miRNAs) from intragenic regions in the *Brassica rapa* and *Brassica oleracea* genomes

miRNA	Origin	Genomic position of MIR gene	Gene	Genomic position of gene
bra-miR168aa	AA	A06:25071508:25071627:+	Bra025084	A06:25069833:25071633:+
bra-miR1885ba	AA	A09:9609771:9609885:−	Bra027889	A09:9609661:9610645:−
bol-miR156aja	CC	C04:9177882:9178079:−	Bol011022	C04: 9176952:9178238:+
bna-miR156zb	CC	C08:34060384:34060507:+	Bol045760	C08: 34060441:34062171:+
bna-miR159e	CC	C07:33256923:33257126:+	Bol039993	C07:33253709:33257013:+
bna-miR172o	CC	C02:7873514:7873656:−	Bol015478	C02:7873505:7874864:−
bna-miR393ha	CC	C08:31301749:31301918:−	Bol044461	C08:31301561:31303832:−
bna-miR827bb	CC	C08:32035435:32035550:+	Bol045592	C08:32035514:32035801:+
bna-novel_miRX328.1[b]	AA	A01:17740853:17741144:+	Bra031407	A01:17740958:17742805:+
bna-novel_miRX9.1[b]	AA	A06:2097964:2098204:−	Bra018766	A06:2096989:2098129:−
bna-novel_miRX54.1[b]	AA	A07:3763334:3763620:−	Bra015071	A07:3763464:3763948:+
bna-novel_miRX71.1[a]	AA	A08:19153262:19153449:−	Bra016582	A08:19150824:19153760:−
bna-novel_miRX265.1[a,b]	AA	A09:26762523:26762830:+	Bra007001	A09:26762518:26762760:+
bna-novel_miRX274.1[a]	AA	A04:12484007:12484137:−	Bra035730	A04:12483056:12484287:−
bna-novel_miRX210.1	AA	A08:9133113:9133260:−	Bra035208	A08:9133176:9134423:−
bna-novel_miRX29.1	CC	C01:2482499:2482576:−	Bol013635	C01:2481297:2482667:−
bna-novel_miRX200.1	CC	C01:3953990:3954264:−	Bol018018	C01:3953521:3954994:+
bna-novel_miRX329.2	CC	C03:20968822:20968968:−	Bol035503	C03:20968783:20969189:−
bna-novel_miRX30.1	CC	C06:45447675:45447793:+	Bol033635	C06:45446556:45448816:−
bna-novel_miRX18.1[b]	CC	C06:45750782:45751017:+	Bol033672	C06:45749418:45750819:+
bna-novel_miRX9.2[a,b]	CC	C07:26238379:26238656:−	Bol016740	C07:26237529:26238523:+
bna-novel_miRX125.1	CC	C09:34092237:34092322:+	Bol030377	C09:34092222:34092668:+
bna-novel_miRX268.1[b]	CC	C04:7137981:7138132:−	Bol016216	C04:7138065:7140536:−

[a]miRNAs located in their target genes.
[b]miRNAs partially located in protein-coding genes.

NBS-LRR disease resistance protein, Myeloblastosis (MYB) family proteins and Kelch repeat-containing F-box protein, respectively. Also, several *Brassica* genus-conserved miRNAs, including miR5716, miR5721, miR6029, miR6030 and miR6035, were predicted to target genes encoding polygalacturonase, biotinyl-lipoyl-containing protein, subtilase, disease resistance proteins and phospatase, respectively. In contrast, the predicted targets of eight novel miRNAs are involved in diverse cellular and signaling processes, such as calmodulin-binding proteins, ATP-binding cassette (ABC) transporter family proteins, N-acetyltransferase, kinases and ubiquitin-protein ligase (Table 4).

A subset of predicted targets differs from those in the literature (Table 5). miR1511 and miR403 have totally different targets in *B. rapa* and *B. oleracea*. *AGO2*, a target of miR403 as validated in *A. thaliana* (Allen *et al.*, 2005), and CuZnSOD (*CSD1*), a target of miR398 (Dugas & Bartel, 2008), were not identified in this study. This may be because their target regions are in untranslated regions (UTRs) rather than ORFs. In addition, we found that *CSD2* (Sunkar *et al.*, 2006), a target of miR398 validated in *A. thaliana*, has three mismatches and a 1-nt bulge in the alignment of the target–miRNA duplex and was therefore filtered out by our pipeline. miR390 and miR391 both target trans-acting siRNA gene 3 (*TAS3*) in *A. thaliana* (Allen *et al.*, 2005; Fahlgren *et al.*, 2007), but *TAS3* could not be identified as a target for either miR390 or miR391 in this study (Table 5). This may be attributable to incomplete reference genome information.

To validate the miRNA–target interaction, RLM-5′ RACE analysis was performed. Twenty-seven predicted target genes for a representative 13 conserved and six novel miRNAs were selected for RLM-5′ RACE analysis. The majority of predicted target sites for the conserved miRNAs could be validated (Fig. 2, Table 5). miR156 targets SPL family genes with multiple cleavage sites in two transcripts of SPL genes (Bra033671 and Bol005638), and miR171 targets the scarecrow-like (SCL) transcription factor at the 13th nucleotide position in three transcripts (Bra003311, Bra000375 and Bol037554), which clearly differs from the most common situation where cleavage of 5′ mRNA occurs at the 10th nucleotide position of miRNAs. Also, miR172 targets the TARGET OF EAT (TOE) transcription factor and miR2111 targets both F-box proteins (Bra025251 and Bol042860), all at the 10th position, the same cleavage site frequently observed in *A. thaliana* and maize (*Zea mays*) (Aukerman & Sakai, 2003; Lauter *et al.*, 2005). In contrast to multiple cleavage sites in *B. rapa* (He *et al.*, 2008), miR1885b exhibited only one cleavage site in a TIR-NBS-LRR R gene in the oilseed rape genome (Fig. 2). We also found cleavage sites beyond the predicted target region, for example, the cleavage sites of Bra003311, Bra000375 and Bol037554 for miR171, Bra022685 for miR164, Bra025251 and Bol042860 for miR2111, and Bra033696 for miR395 (data not shown). This may be a result of multi-targeting of a gene by different miRNAs. Only four RLM-5′ RACE reactions for novel miRNAs provided results (Fig. 2; Table 6). Novel_miRX136 targets the *A. thaliana* Fragile fiber 1 (FRA1) homolog (Bol043063), a kinesin involved in the organization of cellulose microfibrils (Zhu & Dixit, 2012), at the 9th position, while novel_miRX332.1,2 cleaves Bol011897, a homolog of a hypothetical protein (EUTSA_v10021964mg) of *Eutrema salsugineum*. Novel_miR259.1,2 and novel_miRX1.1,2

Table 5 Predicted targets of conserved microRNAs (miRNAs) in *Brassica napus*

miRNA family	Origin	Function of predicted targets	Target reported in *Arabidopsis thaliana*	Validated in this study
miR156/157	AA/CC	Squamosa promoter binding-like (SPL) protein	SPL	Yes
miR158	AA/CC	Pentatricopeptide repeat-containing (PPR) protein; GDSL (consensus sequence of Gly, Asp, Ser and Leu) esterase lipase; ATP transporter protein	PPR	
miR159/319	AA/CC	Myeloblastosis (MYB) domain protein; TCP transcription factor	MYB; TCP	Yes
miR160	AA/CC	Auxin response factor (ARF)	ARF	Yes
miR161	AA/CC	Pentatricopeptide repeat-containing (PPR) protein		
miR162	AA/CC	Dicer-liker (DCL)	DCL	
miR164	AA/CC	NAC (NAM, ATAF1, -2 and CUC2) domain transcription factor	NAC transcription factor	Yes
miR165/166	AA/CC	Homeodomain-leucine zipper (HD-ZIP) transcription factor	HD-ZIP transcription factor	
miR167	AA/CC	Auxin response factor (ARF)	ARF	
miR168	AA/CC	Argonaute protein 1 (AGO1)	Argonaute protein 1 (AGO1)	Yes
miR169	AA/CC	SWI2 SNF2 (switch/sucrose nonfermentable)-like protein; ABC-transport protein; transaldolase; PPR	Hoop-associated protein 2 (HAP2) transcription factor	
miR171	AA/CC	Scarecrow-like (SCL) transcription factor	SCL	Yes
miR172	AA/CC	TARGET OF EAT (TOE) transcription factor; apetala transcription factor (AP2)	TOE; AP2	Yes
miR390	AA/CC	Leucine-rich repeat (LRR) transmembrane protein kinase	Trans-acting siRNA gene 3 (TAS3)	
	AA	Inactive rhomboid protein 1-like		
	CC	Serine threonine-protein kinase		
miR391	AA/CC	Flavin adenine dinucleotide (FAD)-binding and berberine bridge enzyme (BBE)- domain-containing protein; trichome birefingence-like 18 protein	TAS3	
	AA	Phosphatase 2c		
	CC	Uracil 5′-diphosphate (UDP) glucose dehydratase		
miR393	AA/CC	F-box protein	F-box protein	
miR394	AA/CC	F-box protein	F-box protein	Yes
miR395	AA/CC	ATP sulfurylase (APS)	APS; Arabidopsis sulfate transporter (AST)	Yes
miR396	AA/CC	PPR; disease resistance protein; tropine dehydrogenase	Growth-regulating factor (GRF)	
miR397	AA/CC	Laccase	Laccase	
miR398	AA/CC	60s ribosomal protein L31	Copper/zinc superoxide dismutase	
miR399	AA/CC	Ubiqutin ligase protein	E2 ubiquiting-conjugating protein	
miR400	AA/CC	Pentatricopeptide repeat-containing (PPR) protein	PPR	Yes
miR403	AA	Tonsoku (TSK)-associating protein	Argonaute (AGO)	
	CC	Restriction type II-like protein		
miR408	AA/CC	L-ascorbate oxidase; basic blue protein	Laccase (LAC); plantacyanin-like (PCL)	Yes
miR472	AA/CC	Nucleotide-binding site leucine-rich repeat (NBS-LRR) disease resistance protein	Coil-coil domain containing (CC)-NBS-LRR-R gene	
miR529	AA/CC	Nitrite transporter; mutation-induced recessive alleles (mlo)-like protein; peroxidase ATP8a; ACYL synthetase	SPL	
miR827	AA	Cryptic precocious	SYG1/Pho81/XPR1 domain-containing protein (SPX)/zinc finger	
miR845	AA/CC	Solute carrier family; nitrate transporter		
miR858	AA/CC	MYB transcription factor	MYB transcription factor	
miR860	AA/CC	40s ribosomal protein S11	Indole-3-acetic acid (IAA) transcription factor*	
miR1140	CC	Pyridoxal phosphate (PLP)-dependent transferases LRR transmembrane protein kinase	Large-conductance mechanosensitive channel protein*	
miR1439	AA/CC	Kelch repeat-containing F-box protein		
miR1511	AA	GDSL esterase lipase; serine acetyltransferase	GAI (GIBBERELLIC ACID INSENSITIVE), RGA (REPRESSOR of GAI) and SCR (SCARECROW)-domain containing transcription factor	

Table 5 (Continued)

miRNA family	Origin	Function of predicted targets	Target reported in *Arabidopsis thaliana*	Validated in this study
	CC	Neurochondrin protein		
miR1533	AA/CC	Ribonucleic acid (RNA)-binding protein	Su(var)3–9, E(z), Trithorax (SET) domain protein	
miR1863	AA/CC	Pre-mRNA-splicing factor ATP-dependent RNA helicase PRP16; ankyrin repeat-containing protein	1-aminocyclopropane-1-carboxylic oxidase (ACC) oxidase 1*	
miR1885	AA/CC	NBS-LRR) disease resistance protein	NBS-LRR disease resistance protein	Yes
miR2111	AA/CC	Kelch repeat-containing F-box protein	F-box protein	Yes
miR3448	AA/CC	Leucine-rich repeat receptor protein		
miR3630	AA/CC	Toll/interleukin receptor domain-containing (TIR) disease resistance protein		
miR4414	AA/CC	Helix-loop-helix protein; E3 Ubiquitin-fold modifier 1 (UFM1) protein ligase 1		
	AA	Zinc ion-binding protein		
	CC	Homeobox-leucine zipper protein		
miR5024	AA/CC	Arf GTPase-activating protein (ARF-GAP); SAC3/GANP/Nin1/mts3/eIF-3 p25 family		
	AA	Serine carboxypeptidase		
	CC	PPR protein; acyl-CoA synthetase		
miR5067	AA/CC	ATP-binding cassette (ABC) transporter protein; C2H2 zinc finger protein		
	AA	2-oxoglutarate-dependent dioxygenase		
	CC	Esterase lipase thioesterase; glycosyl hydrolase; dead-box ATP-dependent RNA helicase		
miR5654	AA/CC	Pentatricopeptide repeat-containing (PPR) protein	MYB21	
miR5716	AA/CC	Polygalacturonase; Rossmann-fold nicotinamide adenine dinucleotide (NAD)-binding protein		
miR5721	AA/CC	Biotinyl-lipoyl containing protein; Period circadian protein homolog 1 (Per1)-like protein		
miR6028	AA/CC	Naphthoate synthase; senescence-associated protein	Ketoacyl-CoA synthase	
miR6029	AA/CC	Subtilisin-like serine endopeptidase protein; subtilase; eeportin 1a	VirE2-interacting protein 1 (VIP1)*	
miR6030	AA/CC	Disease resistance protein		
miR6035	AA/CC	Embryo defective 1303 protein; phosphatase SGT1a		

*Reported or validated in other plants.

both exhibited multiple cleavage sites that differ from the prediction.

Identification of miRNAs responsive to *V. longisporum* infection

To identify *V. longisporum*-responsive miRNAs, a comparison of the abundance of miRNAs between two libraries (UR and IR) was carried out. The level of an individual miRNA was normalized by total reads in the corresponding library, giving the level of transcript per million (TPM) reads. miRNAs with > 5 TPM were chosen for further analysis and miRNAs with > 100% TMP increase or decrease by comparison were considered to be up- or down-regulated, respectively (Hsieh *et al.*, 2009). We found 62 miRNAs with altered abundances in the *V. longisporum*-infected roots (Fig. 3). The majority of miRNAs (59) were down-regulated, including members of the miR168, miR160, miR169, miR167, miR319, miR390 and miR5654 families and seven novel miRNAs, while only three miRNAs were up-regulated, which all belonged to the miR1885 family (Fig. 3).

As revealed by GO assignments, the genes targeted by responsive miRNAs are involved in regulation of diverse biological (53%), cellular (46.9%) and signaling (23.1%) processes (Table S12). Nineteen genes targeted by miR164, miR168, miR1885 and miR5654, respectively, directly participate in plant immunity and defense against fungal infection, suggesting their functional relevance. Five conserved miRNA families (miR160a,c–n, miR164a,g–i, miR168g–i, miR319a–e and miR1885a–c) representing 28 miRNAs and four novel miRNA families (novel_miRX1.1,2, novel_miRX65.1, novel_miRX249.1,2 and novel_miRX332.1,2) representing seven miRNAs (Fig. 3; Tables S12, S13) were selected for further analysis.

Levels of selected miRNAs were determined at two infection stages by RT-qPCR (Fig. S6). Consistent with the deep sequencing, miR168g–i, miR160a,c–n and miR319a–e were down-regulated at 6 dpi while miR1885a–c exhibited strong up-regulation. Notably, the levels of all selected conserved miRNAs were increased in 12-dpi roots, except for miR164a,g–i, the expression of which was first up-regulated at 6 dpi, rather than being suppressed, and then slightly declined to a level similar to that in the control at 12 dpi. Novel_miRX249.1,2 were

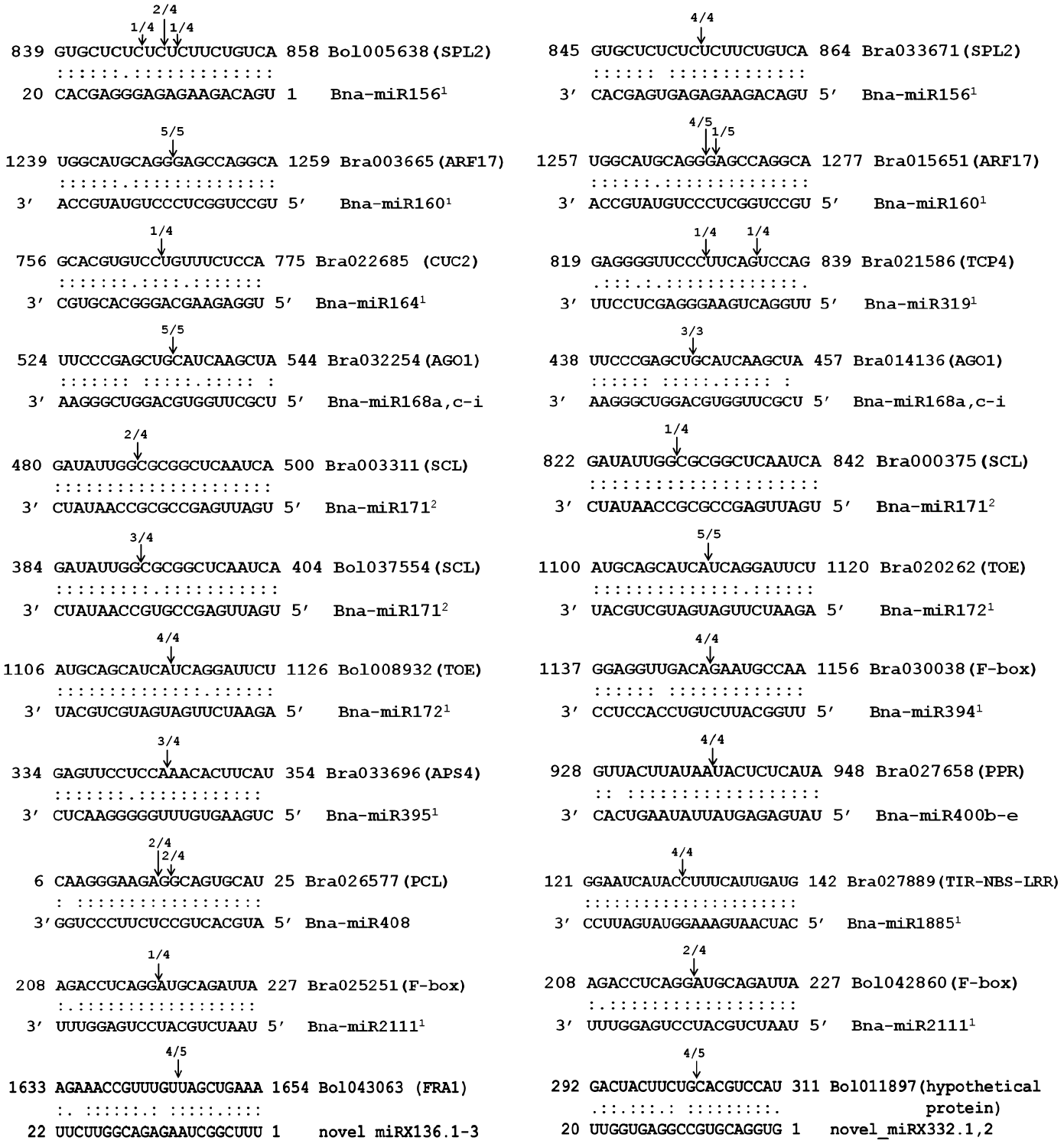

Fig. 2 Validation of predicted microRNA (miRNA) targets using RNA ligase-mediated 5′ rapid amplification of cDNA ends (RACE) PCR. The authentic targets validated here are from *Brassica napus*, and are homologs of genes listed in this figure. The sequences depict the miRNA binding site within the target transcript. The numbers above sequences indicate the detected cleavage site of independent clones. The miRNA and its targets are labeled on the right. [1]All members of miRNA families identified in this study. [2]Except miR171k.

significantly down-regulated in both 6-dpi and 12-dpi roots, consistent with the deep-sequencing data. Novel_miRX1.1,2 and novel_miRX65.1 were both slightly suppressed at 6 dpi but up-regulated at 12 dpi, while novel_miRX332.1,2 showed stable expression (Fig. S6).

We next decided to investigate the effect of the abundance of miRNAs on their target gene expression for five differentially expressed conserved miRNAs (Fig. 4). The levels of miRNAs and their target gene expression were simultaneously determined in 6- and 12-dpi roots. All the selected miRNA–target pairs

Table 6 Predicted targets of novel microRNAs (miRNAs) from *Brassica napus*

miRNA family	Origin	Function of predicted targets	Validated in this study
Novel_miRX1	AA	L-type lectin-containing receptor kinase; RNA pseudourine synthase 6	
	CC	Ubiquitin extension protein; beta-carotene hydroxylase; chitinase	Yes
Novel_miRX65	CC	Predicted protein similar to XP_002869254.1	
Novel_miRX78	AA	Pentatricopeptide repeat-containing protein	
Novel_miRX136	AA/CC	ATP-binding cassette (ABC) transporter family protein	
	AA	N-acetyltransferase	
	CC	Kinesin-like protein	Yes
Novel_miRX249	AA/CC	Delta 1-pyrroline-5-carboxylate synthetase	
	AA	Mitochondrial glycoprotein family protein; tRNA synthetase class I family	
	CC	Nucleoside diphosphate kinase-like protein; heat shock protein-like protein	
Novel_miRX259	AA/CC	Ethylene insensitive 3 family protein; ubiquitin-protein ligase; L-ascorbate peroxidase	
	AA	Calmodulin-binding protein-like protein; endonuclease III-like; polygalacturonase; seryl-tRNA synthetase; pectin lyase-like protein	Yes
	CC	Non-long terminal repeat (non-LTR) retroelement reverse transcriptase; transposase-like protein; ATP synthase epsilon chain	
Novel_miRX290	AA	Glyceraldehyde-3-phosphate dehydrogenase; calmodulin-binding protein	
Novel_miRX332	CC	Hypothetical protein	Yes

exhibited clear reciprocal changes in their expression levels as compared with the controls, whereby an increase or decline in miRNA abundance in roots from 6 to 12 dpi was accompanied by a reciprocal alteration in the expression level of the target gene (Fig. 4). These data provide evidence for direct miRNA–target expression modulations occurring in the plant–*Verticillium* interaction.

miR168/AGO1 expression modulation is involved in the compatible plant–*V. longisporum* interaction

miR168/AGO1 expression modulations have been demonstrated in several studies, and the corresponding knockout mutants are available. A strong suppression of miR168 with a simultaneous increase in AGO1 transcript abundance in the 6-dpi roots (Fig. 4) implies a crucial role of AGO1 in the plant–fungus interaction. To demonstrate this, we challenged the *A. thaliana ago1* knockout mutant *ago1-t*, AGO1 loss-of-function mutants *ago1-25* and *ago1-27*, both carrying a point mutation in the P-element induced wimpy testis (PIWI) domain (Morel *et al.*, 2002), and *mir168b* knockout mutant plants with *V. longisporum* and compared these with wild-type controls. Although slight differences in morphology and growth rate between Columbia (Col-0) wild-type and mutant plants were visible (Fig. 5), they were all severely infected by the fungus (Fig. 5b). Four weeks after infection, typical disease symptoms (stunted growth, reduced rosette diameter and tissue necrosis) were visible in the wild-type and *mir168b* mutant plants (Fig. 5a), and a large number of these plants died as a result of the infection (Fig. 5a). The infected *ago1* mutant plants showed a slight reduction in growth compared with the control, but all three mutants exhibited resistance, with significantly reduced disease symptoms, and the majority of infected plants survived even 4 wk after infection (Fig. 5a). Consistent with this observation, a dramatic increase in fungal biomass was observed in Col-0 and *mir168b* mutant plants but not in *ago1-t*, *ago1-25* and *ago1-27* mutant plants, in which fungal development showed a tendency to plateau (Fig. 5b). These data demonstrate that knockout or loss of function of AGO1 impedes *V. longisporum* development in plants, suggesting an indispensable role of AGO1 in the plant–fungus interaction. We propose that the enhancing of AGO1 expression via suppression of miR168 expression at early infection stages may be a virulence mechanism of *V. longisporum* for colonization of its host. Characterizations of further miRNAs identified in this study are in progress.

Discussion

Brassica rapa and *B. oleracea* genomes facilitate miRNA identification in *B. napus*

To our knowledge, this is the first large-scale study of miRNAs in *B. napus* based on the genomes of its two progenitors. This strategy proved to be efficient and accurate for the identification of miRNAs. We could map > 50% of total reads, representing *c.* 45% of unique reads, to the AA or CC genome, while only 7.14–10.25% of unique reads could be matched by use of EST and TC sequences of *B. napus* (Zhou *et al.*, 2012). By use of available bacterial artificial chromosome (BAC) clones or genome survey sequence (GSS) data for *Brassica* species, the match rate could increase to 15% (Körbes *et al.*, 2012; Xu *et al.*, 2012; Zhao *et al.*, 2012). Recently, Huang *et al.* (2013) identified a set of miRNA candidates or variant sequences in the *B. napus* genome and Lukasik *et al.* (2013) and Wang *et al.* (2013) reported a new set of miRNAs of *B. oleracea*, from which 206 conserved and 60 novel miRNAs are included in our sets.

The number of *B. napus* miRNAs identified in this study is about three times more than that in the model dicot plant *A. thaliana* (299) and significantly higher than in the monocot rice (*Oryza sativa*) (591). This is consistent with the nature of the larger, more complex tetraploid genome of oilseed rape (Parkin *et al.*, 2003). The large number of miRNAs in *B. napus* is

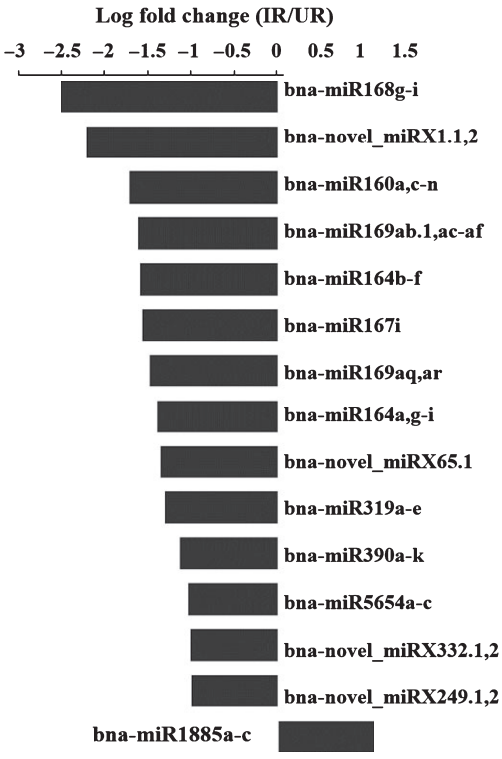

	No. of reads		Log fold change
	UR	IR	
bna-miR168g-i	104182	18466	−2.5
bna-novel_miRX1.1,2	446	97	−2.22
bna-miR160a,c-n	2399	732	−1.73
bna-miR169ab.1,ac-af	1354	444	−1.63
bna-miR164b-f	2199	732	−1.61
bna-miR167i	405	138	−1.57
bna-miR169aq,ar	166	60	−1.49
bna-miR164a,g-i	10479	4005	−1.41
bna-novel_miRX65.1	179	70	−1.37
bna-miR319a-e	111	45	−1.32
bna-miR390a-k	6239	2863	−1.14
bna-miR5654a-c	4878	2401	−1.04
bna-novel_miRX332.1,2	405	202	−1.02
bna-novel_miRX249.1,2	1005	507	−1.01
bna-miR1885a-c	184	406	1.12

Fig. 3 Differentially expressed conserved and novel microRNAs (miRNAs) in libraries from untreated roots (UR; treated with a mock infection) and *V. longisporum*-infected roots (IR). Fold change was calculated using formula: fold change = $\log_2$(miRNA expression in IR/miRNA expression in UR). miRNA expression in each library was normalized to obtain the expression of transcript per million (TPM). Formula for normalization: normalized expression = (actual miRNA count/total count of clean reads) × 1000 000. If the expression level was equal to 0, it was changed to 0.01. If the expression level of miRNA was < 5 in both libraries, it was ignored in the differential expression analysis.

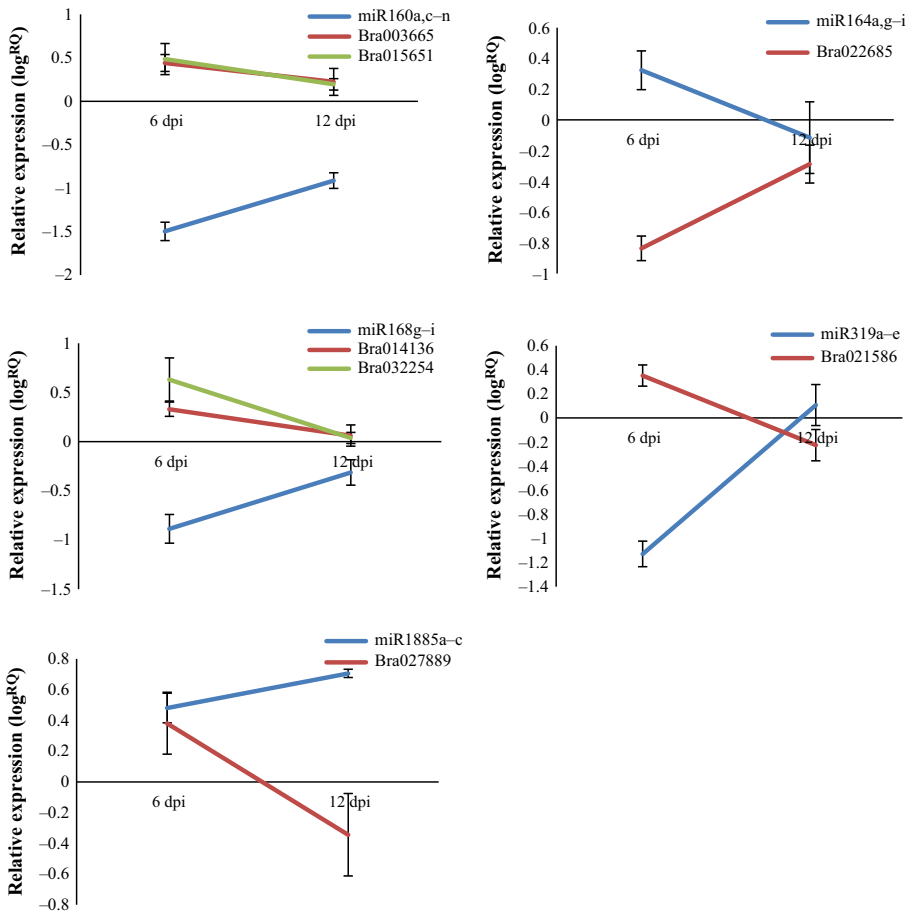

Fig. 4 Quantitative RT-PCR analyses of the abundance of six selected miRNAs and their predicted target genes in response to *Verticillium longisporum* strain VL43 infection in roots of *Brassica napus*. The relative expression level represents the $\log^{RQ}$ value based on the comparative Ct method (Livak & Schmittgen, 2001). Error bars, ± SD. The experiment was repeated three times. dpi, days post-inoculation.

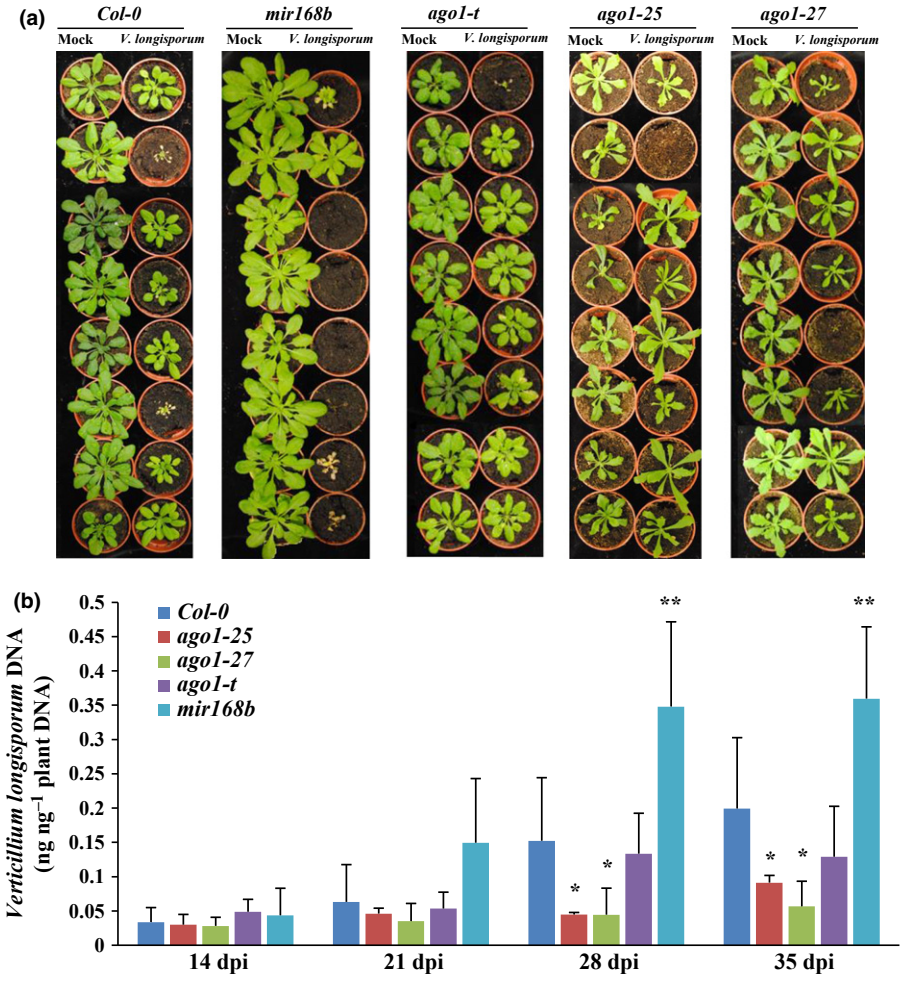

Fig. 5 Analysis of *Arabidopsis thaliana* *mir168b* and *argonaute 1* (*ago1*) mutant (*ago1-t*, *ago1-25* and *ago1-27*) lines in response to *Verticillium longisporum* infection. (a) Symptoms (28 d post-inoculation (dpi)) caused by *V. longisporum* on *mir168b* and *ago1* mutant plants in comparison with the control Columbia (Col-0) plants. Forty plants were used for each investigation. Eight plants are shown here. (b) Quantification of *V. longisporum* DNA in infected plants. Three plants were pooled for each analysis and the experiment was repeated three times. The amount of *V. longisporum* DNA was normalized by dividing by the total *A. thaliana* DNA in the analyzed samples. Error bars, ± 1 SE. An ANOVA was used to determine the significance of the difference between *A. thaliana* mutants and wide-type Col-0 plants (*, $P < 0.05$; **, $P < 0.01$).

obviously attributable to an expansion of miRNAs in the progenitor *Brassica* species as well as in *B. napus* (Fig. S7). As most members of the *B. rapa* and *B. oleracea* miRNA families are well preserved in *B. napus,* the hybridization of *B. rapa* and *B. oleracea* seems to have increased the number of miRNAs in *B. napus* (Table S4). In the case of miR169 (Fig. 6), 26 and 19 members of this family in *B. napus* originated from the AA and CC genomes, respectively; some of these obviously evolved before the *Arabidopsis–Brassica* divergence, but most miR169 sequences originated after the divergence (Fig. 6). The discrepancy in the numbers of the miR169 family between AA and CC genomes suggests that miRNA duplication events had independently occurred in the ancient parental *B. rapa* and *B. oleracea* genomes but with different intensities. Accordingly, we observed a discrepancy in the attribution of miRNAs between the AA and CC subgenomes. In the case of miR171, of its 10 members only three originated from the CC subgenome and seven from the AA subgenome, and all six members of the bna-novel-miRX339 family originated in the AA subgenome. Unequal genomic/segmental duplications as well as tandem duplications of miRNAs might have greatly contributed to the miRNA expansion in *B. napus*. We identified two clusters of miR169 (Fig. S8), miR169l and miR169f, miR169ai, miR169aj, miR169at and miR169ak, in the AA subgenome and two analog clusters, miR169d and miR169w, miR169al, miR169am, miR169ar and miR169av, in the CC subgenome. Subgenome unique paralog clusters were also identified. For instance, miR156r, miR156s and miR156t all reside within a 1-kb region in the AA subgenome while miR168j, miR168k, miR168l and miR168m are all arranged within a 5-kb region in the CC subgenome. These clusters might be explained by independent tandem gene-level duplications occurring after speciation of *B. rapa* and *B. oleracea c.* 3.7 million yr ago (Parkin *et al.*, 1995; Inaba & Nishio, 2002).

The majority of conserved miRNAs of *B. napus* are AA–CC genome syntenic

The availability of the AA and CC genomes provides the possibility to distinguish the possible origins of *B. napus* miRNAs, allowing insights into the evolution of miRNAs in *B. napus*. To this end, we mapped miRNAs to the *B. rapa* and *B. oleracea* genomes, examined the patterns of sequences that mapped to each genome region and finally determined genomic synteny between the AA and CC genomes by microsynteny analysis using the miRNAs and their flanking coding sequences together, leading to three findings: (1) the *B. rapa* AA and *B. oleracea* CC genomes have donated almost equal numbers of miRNAs (429 and 464) to

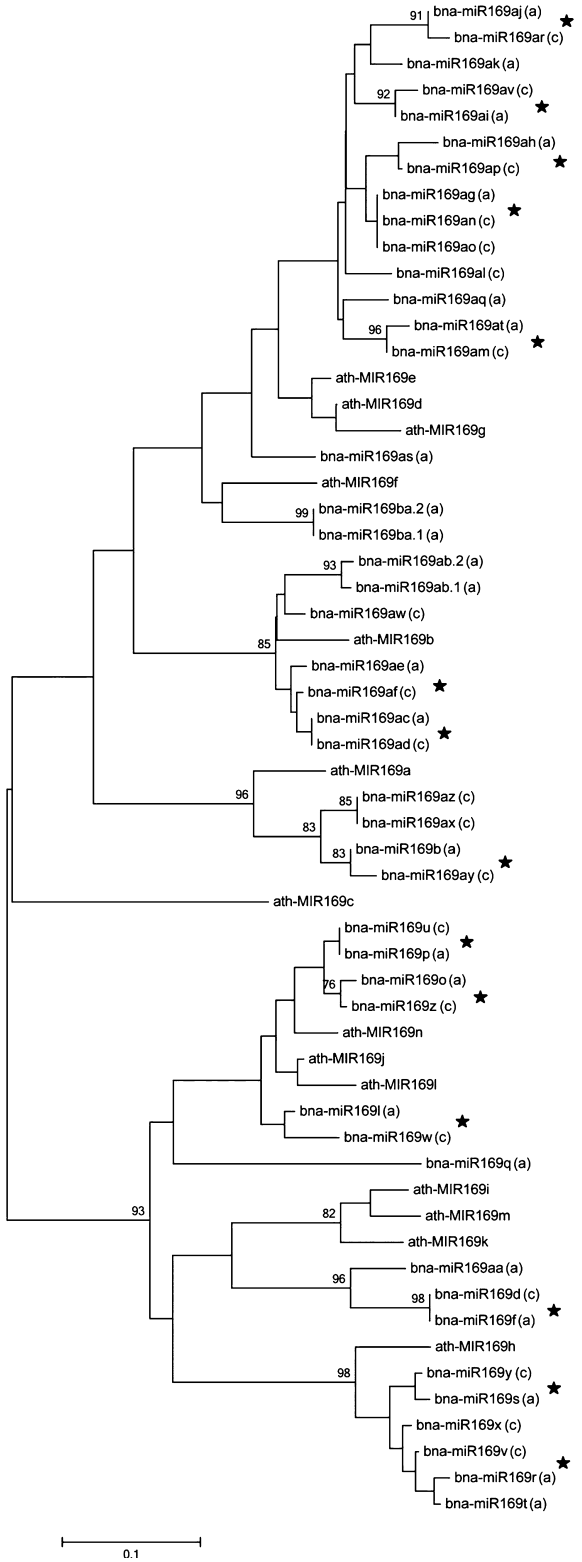

Fig. 6 Phylogenetic tree of members of the miR169 family in *Brassica napus* and *Arabidopsis thaliana* based on their precursor sequences using the neighbor-joining (NJ) method. Bootstrap confidence values were obtained using 1000 replicates and only more than 75% of replications are shown. Putative AA–CC syntenic pairs of miR169 in *B. napus* are labeled with a star. The 'a' or 'c' in parentheses for each microRNA (miRNA) indicates its origins in the AA (*B. rapa*) or CC (*B. oleracea*) genome, respectively.

B. napus, in spite of slight variation in the numbers of conserved and novel miRNAs between the two genomes (Table 3); (2) the majority of the conserved miRNAs (*c.* 68% and 75%, respectively) of the AA and CC subgenomes are syntenic and the AA–CC syntenic pairs are almost evenly distributed throughout the chromosomes of both subgenomes; this synteny is present in most conserved miRNA families, reflecting their ancient but well-conserved functions; and (3) most of the novel miRNAs are AA or CC subgenome-specific. They probably represent 'younger origins', arising after speciation of *B. rapa* and *B. oleracea* independently or alternatively evolving recently after the speciation of *B. napus.* As 'younger' miRNAs are often expressed upon stresses (Fahlgren *et al.*, 2007), the AA or CC subgenome-specific miRNAs identified in this study are interesting candidates for further analysis. However, identification of targets as well as the action modes of novel miRNAs remain a great challenge.

miRNAs responsive to *V. longisporum* infection

The identification of 62 oilseed rape miRNAs responsive to *V. longisporum* infection supports our hypothesis that plant miRNAs are involved in the plant–*V. longisporum* interaction. miRNA–target expression modulations may regulate plant signaling routes trigged by the fungus as part of its colonization strategy (Weiberg *et al.*, 2013) or by the plant for activation of its defense mechanisms. In support of this, the predicted targets are functionally classified as being involved in the regulation of diverse biological and cellular processes and signaling routes. Fourteen genes targeted by miR164, miR168, miR1885 and miR5654, respectively, are involved in plant immunity and five of these targeted by miR164 are active in plant defense against fungal infection (Tables S12, S13). miR160 and miR167 both target ARFs, which control transcription of genes in response to the phytohormone auxin (Ulmasov *et al.*, 1999). As ARFs contribute to antibacterial resistance by repressing auxin signaling (Navarro *et al.*, 2006), the down-regulation of miR160 and miR167 observed in this study might result in an increase in the level of ARFs, which in turn would suppress plant defense responses by enhancing auxin signaling, consequently benefiting fungal colonization. Consistent with this, miR390 was also suppressed in *V. longisporum*-infected roots. Functionally, miR390 targets the *TAS3* gene which down-regulates ARFs (Fahlgren *et al.*, 2007). Thus, it is mostly likely that the ARF-mediated auxin-signaling pathway represents one of the key signaling routes activated by *V. longisporum* to suppress the plant defense response.

Also, miR164 was suppressed in the *V. longisporum*-infected roots. The target of miR164 is *CUP-SHAPED COTYLEDON2* (*CUC2*), belonging to the NAC transcript factor family, which functions in the regulation of plant growth, development and responses to diverse biotic and abiotic stresses (Rhoades *et al.*, 2002). Another target of miR164 is *oresara 1* (*ORE1*) (called ANAC092 or ATNAC2), which acts as a positive regulator of leaf senescence (Kim *et al.*, 2009). Thus, suppression of miR164 leads to an increase in transcript levels of both *CUC2* and *ORE1* in plants, consequently facilitating fungal colonization. Two NAC transcription factors, *VND6* and *VND7*, were shown to be

involved in *V. longisporum*-induced transdifferentiation of *de novo* xylem formation in *A. thaliana* (Rhoades *et al.*, 2002).

miR1885, first reported in *B. rapa* to be induced by TuMV infection (He *et al.*, 2008) and by heat stress (Yu *et al.*, 2012), represents only one highly up-regulated miRNA in the infected roots. The validated target of miR1885 encodes a TIR-NBS-LRR R protein (Bra027889). In contrast to the multiple cleavage sites in *B. rapa* (He *et al.*, 2008), we identified only one cleavage site of miR1885 in its target (a homolog of Bra027889) in oilseed rape. Most interestingly, the target of miR1885 is also the predicted donor of miR1885. Thus, understanding the modulation of the expression of miR1885 and its target may provide new insights into how the fungus suppresses plant R-gene-mediated resistance (Zhai *et al.*, 2011; Li *et al.*, 2012).

Most notably, miR168g–i exhibited the greatest accumulation and were significantly suppressed in the infected roots compared with the control. miR168 interferes with AGO1, which was correspondingly up-regulated in the infected roots. AGO1 is a key component in many miRNA pathways regulating diverse physiological processes (Rhoades *et al.*, 2002; Vaucheret *et al.*, 2004, 2006), including a number of PAMP-triggered immune (PTI) responses (Li *et al.*, 2010). Várallyay *et al.* (2010) reported that, upon cymbidium ringspot (CymRSV) virus infection, the endogenous miR168 level was modulated, leading to attenuation of the antiviral function of the AGO1 protein by inhibition of its translational activity. In this study, clear reciprocal alterations in the abundance of miR168 (suppression) and expression of its target AGO1 (up-regulation) in infected roots as well as the availability of *A. thaliana* knockout mutants prompted us to functionally characterize the role of miRNA168–AGO1 expression modulations in the plant–fungus interaction. We demonstrated that *mir168b* mutant plants exhibited similar susceptibility to the control plants, while all three AGO1 mutants showed resistance with greatly reduced disease symptoms. The finding that both knockout and loss of function of AGO1 impede *V. longisporum* development suggests an indispensable role of AGO1 in the compatible plant–*Verticillium* interaction. This finding is consistent with the observation that *A. thaliana* gene silencing mutants *sgs2*, *sgs3*, *ago7* and *dcl4* exhibited enhanced susceptibility to *V. dahliae*, while the *ago1* mutant showed enhanced resistance (Ellendorff *et al.*, 2009), and is also consistent with the recent report that the fungus *B. cinerea* hijacks the plant's gene silencing mechanism by binding its 'virulent' sRNA effectors to AGO1. The *A. thaliana* AGO1 mutant exhibits reduced susceptibility to *B. cinerea* (Weiberg *et al.*, 2013). It is reasonable to propose that enhancing the expression of AGO1 by suppressing miR168 expression at early infection stages may be a virulence mechanism of *V. longisporum* for colonization of its host. Nevertheless, characterizations of further miRNAs identified in this study are needed to really understand the role of miRNAs in regulating the plant–fungus interaction.

Acknowledgements

We thank Prof. Dr Hervé Vaucheret, Laboratoire de Biologie Cellulaire, INRA, France for providing *A. thaliana ago1-25* and *ago1-27* seeds, and Dr Tim Thurau for his help in the laboratory. This work was financially supported by the Bundesanstalt für Landwirtschaft and Ernährung, Germany (Grant no. 2814IP004) and the National Basic Research Program of China (Grant no. 2011CB109306). The authors thank DAAD and the China Scholarship Council for travel grants (Grant no. 56191966).

References

Allen E, Xie Z, Gustafson AM, Carrington JC. 2005. MicroRNA-directed phasing during trans-acting siRNA biogenesis in plants. *Cell* **121**: 207–221.

Aukerman MJ, Sakai H. 2003. Regulation of flowering time and floral organ identity by a microRNA and its *APETALA2*-like target genes. *Plant Cell* **15**: 2730–2741.

Aung K, Lin SI, Wu CC, Huang YT, Su CL, Chiou TJ. 2006. Pho2, a phosphate over accumulator, is caused by a nonsense mutation in a microRNA399 target gene. *Plant Physiology* **141**: 1000–1011.

Bari R, Pant BD, Stitt M, Scheible WR. 2006. PHO2, microRNA399, and PHR1 define a phosphate-signaling pathway in plants. *Plant Physiology* **141**: 988–999.

Bartel DP. 2004. MicroRNAs: genomics, biogenesis, mechanism, and function. *Cell* **116**: 281–297.

Chen C, Ridzon DA, Broomer AJ, Zhou Z, Lee DH, Nguyen JT, Barbisin M, Xu NL, Mahuvakar VR, Andersen MR *et al.* 2005. Real-time quantification of microRNAs by stem-loop RT-PCR. *Nucleic Acids Research* **60**: 591–602.

Conesa A, Götz S. 2008. Blast2GO: q comprehensive suite for functional analysis in plant genomics. *Internationl Journal of Plant Genomics* **2008**: 619832.

Dai XB, Zhao PXC. 2011. psRNATarget: a plant small RNA target analysis server. *Nucleic Acids Research* **39**: 155–159.

Dugas DV, Bartel B. 2008. Sucrose induction of *Arabidopsis* miR398 represses two Cu/Zn superoxide dismutases. *Plant Molecular Biology* **67**: 403–417.

Ellendorff U, Fradin EF, de Jonge R, Thommal BPHJ. 2009. RNA silencing is required for *Arabidopsis* defence against *Verticillium* wilt disease. *Journal of Experimental Botany* **60**: 591–602.

Eynck C, Koopmann B, Grunewaldt-Stoecker G, Karlovsky P, von Tiedeman A. 2007. Differential interactions of *Verticillium longisporum* and *V. dahliae* with *Brassica napus* detected with molecular and histological techniques. *European Journal of Plant Pathology* **118**: 259–274.

Eynck C, Koopmann B, Karlovsky P, von Tiedemann A. 2009. Internal resistance in winter oilseed rape inhibits systemic spread of the vascular pathogen *Verticillium longisporum*. *Phytopathology* **99**: 802–811.

Fahlgren N, Howell MD, Kasschau KD, Chapman EJ, Sullivan CM, Cumbie JS, Givan SA, Law TF, Grant SR, Dangl JL *et al.* 2007. High-throughput sequencing of *Arabidopsis* microRNAs: evidence for frequent birth and death of *MIRNA* genes. *PLoS ONE* **2**: e219.

Floerl S, Druebert C, Aroud HI, Karlovsky P, Polle A. 2010. Disease symptoms and mineral nutrition in *Arabidopsis thaliana* in response to *Verticillium longisporum* VL43 infection. *Journal of Plant Pathology* **92**: 693–700.

Floerl S, Druebert C, Majcherczyk A, Karlovsky P, Kües U, Polle A. 2008. Defence reactions in the apoplastic proteome of oilseed rape (*Brassica napus* var. napus) attenuate *Verticillium longisporum* growth but not disease symptoms. *BMC Plant Biology* **8**: 129.

Floerl S, Majcherczyk A, Possienke M, Feussner K, Tappe H, Gatz C, Feussner I, Kües U, Polle A. 2012. *Verticillium longisporum* infection affects the leaf apoplastic proteome, metabolome, and cell wall properties in *Arabidopsis thaliana*. *PLoS ONE* **7**: e31435.

He XF, Fang YY, Feng L, Guo HS. 2008. Characterization of conserved and novel microRNAs and their targets, including a TuMV-induced TIR-NBS-LRR class R gene-derived novel miRNA in Brassica. *FEBS Letters* **582**: 2445–2452.

Hewezi T, Maier TR, Nettleton D, Baum TJ. 2012. The *Arabidopsis microRNA396-GRF1/GRF3* regulatory module acts as a developmental regulator in the reprogramming of root cells during cyst nematode infection. *Plant Physiology* **159**: 321–335.

Hsieh LC, Lin SI, Shih ACC, Chen JW, Lin WY, Tseng CY, Li WH, Chiou TJ. 2009. Uncovering small RNA-mediated responses to phosphate deficiency in Arabidopsis by deep sequencing. *Plant Physiology* **151**: 2120–2132.

Huang D, Koh C, Feurtado JA, Tsang EW, Cutler AJ. 2013. MicroRNAs and their putative targets in *Brassica napus* seed maturation. *BMC Genomics* **14**: 140.

Inaba R, Nishio T. 2002. Phylogenetic analysis of Brassiceae based on the nucleotide sequences of the S-locus related gene, SLR1. *Theoretical and Applied Genetics* **105**: 1159–1165.

Iven T, Koenig S, Singh S, Braus-Stronmeyer SA, Bischoff M, Tietze LF, Braus GH, Lipka V, Feussner I, Droege-Laser W. 2012. Transcriptional activation and production of tryptophan-derived secondary metabolites in *Arabidopsis* roots contributes to the defense against the fungal vascular pathogen *Verticillium longisporum*. *Molecular Plant* **5**: 1389–1402.

Iwakawa HO, Tomari Y. 2013. Molecular insights into microRNA-mediated translational repression in plants. *Molecular Cell* **52**: 591–601.

Johansson A, Staal J, Dixelius C. 2006. Early responses in the Arabidopsis-Verticillium longisporum pathosystem are dependent on NDR1, JA- and ET-associated signals via cytosolic NPR1 and RFO1. *Molecular Plant-Microbe Interaction* **19**: 958–969.

Jones-Rhoades MJ, Bartel B, Bartel DP. 2006. MicroRNAs and their regulatory roles in plants. *Annual Review of Plant Biology* **57**: 19–53.

Jones-Rhoades MW, Bartel DP. 2004. Computational identification of plant microRNAs and their targets, including a stress-induced miRNA. *Molecular Cell* **14**: 787–799.

Kasschau KD, Xie Z, Allen E, Llave C, Chapman EJ, Krizan KA, Carrington JC. 2003. P1/HC-Pro, a viral suppressor of RNA silencing, interferes with *Arabidopsis* development and miRNA function. *Developmental Cell* **4**: 205–217.

Kim JH, Woo HR, Kim J, Lim PO, Lee IC, Choi SH, Hwang D, Nam HG. 2009. Trifurcate feed-forward regulation of age-dependent cell death involving *miR164* in *Arabidopsis*. *Science* **323**: 1053–1057.

Körbes AP, Machado RD, Guzman F, Almerao MP, de Oliveira LFV, Loss-Morais G, Turchetto-Zolet AC, Cagliar A, Maraschin FS, Margis-Pinheiro M *et al.* 2012. Identifying conserved and novel MicroRNAs in developing seeds of *Brassica napus* using deep sequencing. *PLoS ONE* **7**: e50663.

Krzywinski M, Schein J, Birolİ Connors J, Gascoyne R, Horsman D, Jones SJ, Marra MA. 2009. Circos: an information aesthetic for comparative genomics. *Genome Research* **19**: 1639–1645.

Laufs P, Peaucelle A, Morin H, Traas J. 2004. MicroRNA regulation of the CUC genes is required for boundary size control in *Arabidopsis* meristems. *Development* **131**: 4311–4322.

Lauter N, Kampani A, Carlson S, Goebel M, Moose SP. 2005. MicroRNA172 down-regulates glossy15 to promote vegetative phase change in maize. *Proceedings of the National Academy of Sciences, USA* **102**: 9412–9417.

Li F, Pignatta D, Bendix C, Brunkard JO, Cohn MM, Tung J, Sun H, Kumar P, Baker B. 2012. MicroRNA regulation of plant innate immune receptors. *Proceedings of the National Academy of Sciences, USA* **109**: 1790–1795.

Li Y, Zhang Q, Zhang J, Wu L, Qi Y, Zhou JM. 2010. Identification of microRNAs involved in pathogen-associated molecular pattern-triggered plant innate immunity. *Plant Physiology* **152**: 2222–2231.

Livak KJ, Schmittgen TD. 2001. Analysis of relative gene expression data using real-time quantitative PCR and the $2^{-\Delta\Delta CT}$ method. *Methods* **25**: 402–408.

Lu S, Sun YH, Amerson H, Chiang VL. 2007. MicroRNAs in loblolly pine (*Pinus taeda L.*) and their association with fusiform rust gall development. *Plant Journal* **51**: 1077–1098.

Lukasik A, Pietrykowska H, Paczek L, Szweykowska-Kulinska Z, Zielenkiewicz P. 2013. High-throughput sequencing identification of novel and conserved miRNAs in the *Brassica oleracea* leaves. *BMC Genomics* **14**: 801.

Ma Z, Coruh C, Axtell MJ. 2010. *Arabidopsis lyrata* small RNAs: transient miRNA and small interfering RNA loci within the *Arabidopsis* genus. *Plant Cell* **22**: 1090–1103.

Mallory AC, Bartel DP, Bartel B. 2005. MicroRNA-directed regulation of Arabidopsis auxin response factor 12 is essential for proper development and modulates expression of early auxin response genes. *The Plant Cell* **17**: 1360–1375.

Morel JB, Godon C, Mourrain P, Béclin C, Boutet S, Feuerbach F, Proux F, Vaucheret H. 2002. Fertile hypomorphic *ARGONAUTE* (*ago1*) mutants impaired in post-transcriptional gene silencing and virus resistance. *Plant Cell* **14**: 629–639.

Naqvi AR, Sarwat M, Hasan S, Roychodhury N. 2012. Biogenesis, functions and fate of plant microRNAs. *Journal of Cellular Physiology* **227**: 3163–3168.

Navarro L, Dunoyer P, Jay F, Arnold B, Dharmasiri N, Estelle M, Voinnet O, Jones JD. 2006. A plant miRNA contributes to antibacterial resistance by repressing auxin signaling. *Science* **312**: 436–439.

Palatnik JF, Allen E, Wu X, Schommer C, Schwab R, Carrington JC, Weigel D. 2003. Control of leaf morphogenesis by microRNAs. *Nature* **425**: 257–263.

Parkin IAP, Sharpe AG, Keith DJ, Lydiate DJ. 1995. Identification of the A and C genomes of the amphidiploid *Brassica napus* (oilseed rape). *Genome* **38**: 1122–1131.

Parkin IAP, Sharpe AG, Lydiate DJ. 2003. Patterns of genome duplication within the *Brassica napus* genome. *Genome* **46**: 291–303.

Qu F, Ye X, Morris TJ. 2008. *Arabidopsis* DRB4, AGO1, AGO7, and RDR6 participate in a DCL4-initiated antiviral RNA silencing pathway negatively regulated by DCL1. *Proceedings of the National Academy of Sciences, USA* **105**: 14732–14737.

Ralhan A, Schöttle S, Thurow C, Iven T, Feussner I, Polle A, Gatz C. 2012. The vascular pathogen *Verticillium longisporum* requires a jasmonic acid-independent COI1 function in roots to elicit disease symptoms in *Arabidopsis* shoots. *Plant Pathology* **159**: 1192–1203.

Reusche M, Thole K, Janz D, Truskian J, Rindfleisch S, Druebert C, Polle A, Lipka C, Teichmann T. 2012. *Verticillium* infection triggers vascular-related NAC domain7-dependent *de novo* xylem formation and enhances drought tolerance in *Arabidopsis*. *The Plant Cell* **24**: 3823–3837.

Rhoades MW, Reinhart BJ, Lim LP, Burge CB, Bartel B, Bartel DP. 2002. Prediction of plant microRNA targets. *Cell* **110**: 513–520.

Rietz S, Bernsdorff FEM, Cai D. 2012. Members of the germin-like protein family in *Brassica napus* are candidates for the initiation of an oxidative burst that impedes pathogenesis of *Sclerotinia sclerotiorum*. *Journal of Experimental Botany* **63**: 5507–5519.

Singh S, Braus-Stromeyer SA, Timpner C, Valerius O, von Tiedemann A, Karlovsky P, Druebert C, Polle A, Braus GH. 2012. The plant host *Brassica napus* induces in the pathogen *Verticillium longisporum* the expression of functional catalase peroxidase which is required for the late phase of disease. *Molecular Plant-Microbe Interaction* **25**: 569–581.

Sunkar R, Kapoor A, Zhu JK. 2006. Posttranscriptional induction of two Cu/Zn superoxide dismutase genes in *Arabidopsis* is mediated by down regulation of miR398 and important for oxidative stress tolerance. *Plant Cell* **18**: 2051–2065.

Thompson JD, Higgins DG, Gibson TJ. 1994. CLUSTALW: improving the sensitivity of progressive multiple sequence alignment through sequence weighting, position-specific gap penalties and weight matrix choice. *Nucleic Acids Research* **22**: 4673–4680.

Ulmasov T, Hagen G, Guilfoyle TJ. 1999. Dimerization and DNA binding of auxin response factors. *Plant Journal* **19**: 309–319.

Várallyay E, Válóczi A, Agyi A, Burgyán J, Havelda Z. 2010. Plant virus-mediated induction of miR168 is associated with repression of ARGONAUTE1 accumulation. *EMBO Journal* **29**: 3507–3519.

Vaucheret H, Mallory AC, Bartel DP. 2006. AGO1 homeostasis entails coexpression of *MIR168* and *AGO1* and preferential stabilization of miR168 by AGO1. *Molecular Cell* **22**: 129–136.

Vaucheret H, Vazquez F, Crété P, Bartel DP. 2004. The action of ARGONAUTE1 in the miRNA pathway and its regulation by the miRNA pathway are crucial for plant development. *Genes & Development* **18**: 1187–1197.

Vazquez F, Legrand S, Windels D. 2010. The biosynthetic pathways and biological scopes of plant small RNAs. *Trends in Plant Science* **15**: 337–345.

Veronese P, Narasimhan ML, Stevenson RA, Zhu JK, Weller SC, Subbarao KV, Bressan RA. 2003. Identification of a locus controlling *Verticillium* disease symptom response in *Arabidopsis thaliana*. *Plant Journal* **35**: 574–587.

Voinnet O. 2009. Origin, biogenesis, and activity of plant microRNAs. *Cell* **136**: 669–687.

Wang F, Li H, Zhang YH, Li JJ, Li LB, Liu LF, Wang LH, Wang CH, Gao JW. 2013. MicroRNA expression analysis of rosette and folding leaves in Chinese cabbage using high-throughput Solexa sequencing. *Gene* **532**: 222–229.

Wang X, Wang H, Wang J, Sun R, Wu J, Liu S, Bai Y, Mun JH, Bancroft I, Cheng F *et al.* 2011. The genome of the mesopolyploid crop species *Brassica rapa*. *Nature Genetics* **43**: 1035–1039.

Weiberg A, Wang M, Lin FM, Zhao H, Zhang Z, Kaloshian I, Huang HD, Jin H. 2013. Fungal small RNAs suppress plant immunity by hijacking host RNA interference pathways. *Science* **342**: 118–123.

Wu MF, Tian Q, Reed JW. 2006. *Arabidopsis microRNA167* controls patterns of *ARF6* and *ARF8* expression, and regulates both female and male reproduction. *Development* **133**: 4211–4218.

Xu MY, Dong Y, Zhang QX, Zhang L, Luo YZ, Sun J, Fan YL, Wang L. 2012. Identification of miRNAs and their targets from *Brassica napus* by high-throughput sequencing and degradome analysis. *BMC Genomics* **13**: 421.

Yu X, Wang H, Lu YZ, Ruiter M, Cariaso M, Prins M, Tunen A, He Y. 2012. Identification of conserved and novel microRNAs that are responsive to heat stress in *Brassica rapa*. *Journal of Experimental Botany* **63**: 1025–1038.

Zeise K, von Tiedemann A. 2002. Host specialization among vegetative compatibility groups of *Verticillium dahliae* in relation to *Verticillium longisporum*. *Journal of Phytopathology* **150**: 112–119.

Zhai J, Jeong DH, De Paoli E, Park S, Rosen BD, Li Y, González AJ, Yan Z, Kitto SL, Grusak MA *et al.* 2011. MicroRNAs as master regulators of the plant NB-LRR defense gene family via the production of phased, trans-acting siRNAs. *Genes & Development* **25**: 2540–2553.

Zhao YT, Wang M, Fu SX, Yang WC, Qi CK, Wang XJ. 2012. Small RNA profiling in two *Brassica napus* cultivars identifies microRNAs with oil production- and development-correlated expression and new small RNA classes. *Plant Physiology* **158**: 813–823.

Zhou ZS, Song JB, Yang ZM. 2012. Genome-wide identification of *Brassica napus* microRNAs and their targets in response to cadmium. *Journal of Experimental Botany* **63**: 4597–4613.

Zhu C, Dixit R. 2012. Functions of the *Arabidopsis* kinesin superfamily of microtubule-based motor proteins. *Protoplasma* **249**: 887–899.

Supporting Information

Additional supporting information may be found in the online version of this article.

Fig. S1 Distribution of sequence reads in *Brassica napus* small RNA libraries made from untreated (UR) and *V. longisporum*-infected (IR) roots.

Fig. S2 Nucleotide preferences at each position of the sequences identified as *Brassica napus* small RNAs.

Fig. S3 Expression of several miRNAs and their corresponding miRNA*s.

Fig. S4 Validation of identified conserved and novel miRNAs by stem-loop reverse transcription PCR.

Fig. S5 Sequence alignments of three tandemly duplicated miRNA clusters.

Fig. S6 Quantitative RT-PCR analysis of selected miRNAs in *B. napus* roots after infection with *V. longisporum* strain VL 43.

Fig. S7 Comparison of numbers of members of some conserved miRNA families between *Arabidopsis thaliana* (according to miRBase release 20) and *Brassica napus* (miRNAs identified in this study plus miRNA records in miRBase).

Fig. S8 A model to explain the two paralog clusters of miR169.

Table S1 Primers used in miRNA expression analysis

Table S2 Quantitative RT-PCR primers for target genes used in this study

Table S3 RLM-5′ RACE primers used in this study

Table S4 List of all identified conserved miRNAs in this study

Table S5 List of all identified novel miRNAs in this study

Table S6 Microsyntenic analysis of conserved miRNAs identified in this study

Table S7 Microsyntenic analysis of novel miRNAs identified in this study

Table S8 Predicted targets of conserved miRNAs from *B. rapa* transcripts

Table S9 Predicted targets of conserved miRNAs from *B. oleracea* transcripts

Table S10 Predicted targets of novel miRNAs from *B. rapa* transcripts

Table S11 Predicted targets of novel miRNAs from *B. oleracea* transcripts

Table S12 Functional classification of different expressed conserved miRNA targets with miRNA based on gene ontology (GO)

Table S13 Functional classification of different expressed novel miRNA targets with miRNA based on gene ontology (GO)

Please note: Wiley Blackwell are not responsible for the content or functionality of any supporting information supplied by the authors. Any queries (other than missing material) should be directed to the *New Phytologist* Central Office.